NASA TECHNICAL NOTE

NASA TN D-2763

NASA TN D-2763

PARAMETRIC STUDY OF A THERMOELECTROSTATIC GENERATOR FOR SPACE APPLICATIONS

by Paul M. Margosian

Lewis Research Center

Cleveland, Ohio

NATIONAL AERONAUTICS AND SPACE ADMINISTRATION • WASHINGTON, D. C. • APRIL 1965

NASA TN D-2763

PARAMETRIC STUDY OF A THERMOELECTROSTATIC GENERATOR FOR SPACE APPLICATIONS

By Paul M. Margosian

Lewis Research Center
Cleveland, Ohio

NATIONAL AERONAUTICS AND SPACE ADMINISTRATION

For sale by the Clearinghouse for Federal Scientific and Technical Information
Springfield, Virginia 22151 – Price $2.00

PARAMETRIC STUDY OF A THERMOELECTROSTATIC GENERATOR FOR SPACE APPLICATIONS

by Paul M. Margosian

Lewis Research Center

SUMMARY

Examined in this report is the theoretical performance of a thermoelectrostatic generator, which is a variable capacitance device capable of converting thermal energy directly to electrical energy. Two physically realizable thermodynamic cycles were selected. Two dielectric materials, barium titanate and polyethylene terephthalate (Mylar), were selected for their potential ability to yield the best performance attainable with this device. Mathematical expressions for internal energy and entropy in terms of electrical and thermodynamic parameters were derived. Mathematical approximations to the behavior of the dielectric constants of the materials were chosen. Equations describing the thermodynamic cycles were derived and solved numerically. The upper limits on performance were found to be the following: maximum thermal efficiency, 1 to 4 percent; and maximum energy output, 0.5 to 1.5 joules per cubic centimeter of dielectric per cycle. Realistic performance, dictated by material properties and limitations on the electric field that can be supported, is lower by at least a factor of five.

For use in space an electrical generator should have minimum weight. In order to evaluate this parameter, the heat-transfer equations were written for a typical design, heated by the sun or by a nuclear reactor, and solved numerically. Combining the results of the thermodynamic and the heat-transfer calculations led to an estimated minimum specific weight of the order of 50 to 150 pounds per kilowatt.

INTRODUCTION

Lightweight sources of electrical power are essential for the performance of almost any mission in space. Power requirements range from a few watts for communication with near-Earth satellites to several megawatts for a Mars mission employing electric propulsion (ref. 1).

An attractive method of producing electric power in space is the direct conversion of thermal energy, such as solar radiation or heat from a nuclear reactor, to electric energy. One such method is the thermoelectrostatic gener-

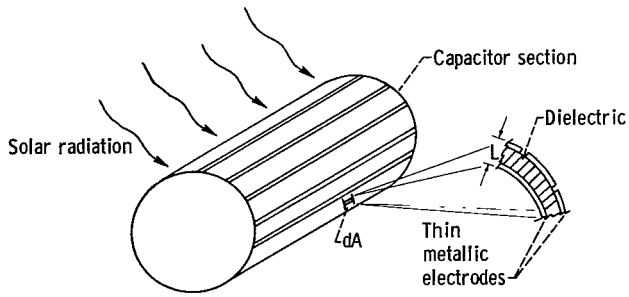

(a) Schematic of generator.

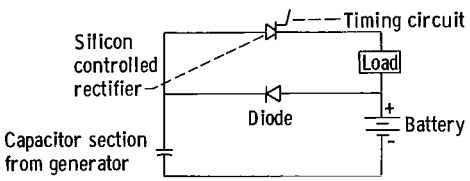

(b) Sample circuit for executing cycle A.

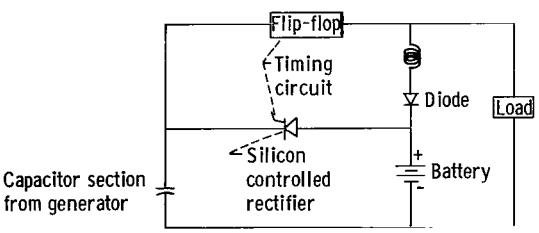

(c) Sample circuit for executing cycle B.

Figure 1. - Electrical and mechanical details of one possible design for thermoelectrostatic generator.

ator (ref. 2) discussed in this report.

The principle of operation of this device is best illustrated by considering a simple version, such as a parallel plate capacitor made from a material whose dielectric constant varies with temperature. The charge on such a capacitor is given by the product of capacitance and voltage. The dielectric constant can be decreased by either increasing or decreasing the temperature depending on the material employed. If the capacitance is decreased by changing the temperature of the dielectric while charge is held constant, the voltage on the capacitor must increase. Since the electric energy stored in the capacitor is proportional to the product of charge and voltage, it will also increase. Some of the thermal energy transferred in changing the temperature of the dielectric has been converted to electric energy.

Like any heat engine, this device may be analyzed by standard thermodynamic techniques. The usual expressions for internal energy and entropy must be modified to take into account the fact that electric and thermodynamic parameters are equally important in determining the performance of the generator.

For the sake of simplicity, the two thermodynamic cycles considered are made up of processes in which one of the parameters of charge, electric field, or entropy is held constant. Cycles including isothermal processes were considered impractical for space application because of the necessity of some sort of uniform rotation of the generator with respect to the radiant heat source (sun or reactor) in order to alternately heat and cool it. The continuously varying heat flux would make execution of an isothermal process difficult. Other possible cycles have been omitted on the grounds of lower efficiency or of impracticality.

The dielectrics were selected on the basis of their potential for yielding the best possible performance for this generator. In order to keep the analysis as straightforward as possible, it is desirable to find simple mathematical approximations to the behavior of these materials. The approximations

used were selected on the basis of information available in the literature.

The output parameters, thermal efficiency and energy output per unit volume of dielectric per cycle, were calculated as functions of maximum and minimum temperatures and electrical parameters. In order to arrive at the final parameter of interest (specific weight), it was necessary to select a specific design. The design selected is cylindrical (fig. 1(a)) and could be heated by either the sun or a nuclear reactor. The heat-transfer equations were written for this design and solved numerically. This calculation gave the maximum and minimum temperatures as functions of the number of cycles executed per second and of the amount of dielectric material employed. The results of the thermodynamic and the heat-transfer calculations were combined to yield estimates of specific weight for this generator.

ANALYSIS

Basic Theory

Energy in a variety of forms can be converted to electric energy by means of a variable capacitance device (all symbols are defined in appendix A). A parallel plate capacitor C_1 is initially charged to a potential V_1 so that the charge q on the capacitor becomes

$$q = C_1 V_1 \tag{1}$$

while the electrical energy initially stored is

$$W_1' = \frac{1}{2} q V_1 \tag{2}$$

The source of the charge is then removed. The charge will remain constant while the capacitance is changed to a new value C_2 by adding or rejecting heat. These conditions yield the new voltage

$$V_2 = \frac{C_1}{C_2} V_1 \tag{3}$$

and a new electrical energy

$$W_2' = \frac{1}{2} q V_2 \tag{4}$$

The net change in stored electric energy is

$$W_2' - W_1' = \frac{1}{2} q V_1 \left(\frac{C_1}{C_2} - 1 \right) \tag{5}$$

which represents an increase of $C_2 < C_1$. Thus, some portion of the energy expended in decreasing the capacitance is converted to electrical energy.

For parallel plates, capacitance is given by

$$C = \frac{A\epsilon\epsilon_o}{L} \tag{6}$$

which indicates that capacitance can be varied by changing either the geometry (for example, by forcing the plates apart and thereby doing mechanical work against the field) or the dielectric constant. Electrostatic generators, which convert mechanical energy to electric energy by varying the geometry of capacitors, have been constructed and are discussed in the literature (refs. 3 to 6). If a dielectric material whose permittivity is a function of temperature is employed, electric energy can be produced by varying the temperature of the material; that is, thermal energy can be converted directly to electric energy. A generator operating on this principle can be analyzed by standard thermodynamic methods by selecting a suitable thermodynamic cycle.

Thermodynamic Cycles

In selecting a thermodynamic cycle, it is necessary to strive for physical realizability and best possible thermal efficiency. An essential requirement for space application is minimum specific weight; this requires the maximum possible energy output per unit volume of dielectric per cycle. Because of the necessity for minimum weight, it is desirable that the auxiliary equipment needed to execute the cycle be as simple as possible. Also, the output voltage should be greater than the input voltage in order that a simple device, such as a battery, can provide the necessary excitation (i.e., initial charge on the capacitor). This excitation device should not be required to deliver any net power over a complete cycle.

One possible generator design is presented in figure 1(a) (from ref. 2). It consists of a solid dielectric in the form of a thin cylindrical film with thin metallic electrode sections on the inner and outer surfaces. Each capacitor section is taken narrow enough that all of it may be considered to be at the same temperature. This device is heated by the sun and rejects heat by radiation; it rotates in order to carry each section through a thermal cycle.

Execution of an isothermal process would be impractical with the rotating cylindrical design; consequently, the use of a Carnot cycle is not feasible. The remaining quantities that can be held constant during a thermodynamic process are charge, voltage (and therefore electric field), and entropy (assuming a lossless dielectric).

On the basis of the previous considerations and ease of analysis, two cycles have been selected for detailed analysis (see fig. 2). The cycles are sketched on a graph of electric field E as a function of electric displacement D because, as will be demonstrated later in the discussion, the area bounded by the cycle is equal to the net electrical work output.

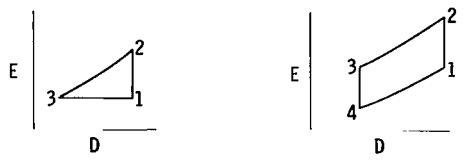

(a) Cycle A. (b) Cycle B.

Figure 2. - Two cycles selected for detailed analysis.

Cycle A (from ref. 2). - An initial charge is placed on the capacitor at an initial field E_1 and an initial temperature T_1 corresponding to a maximum value of the dielectric constant ϵ. At constant charge, the temperature is changed to T_2 so as to reduce ϵ and, by using equations (3) and (6), increase the electric field to E_2. Next the capacitor is discharged (through the load) adiabatically (and isentropically for a lossless dielectric) to the original field E_1. This condition results in a temperature T_3 for which ϵ will be slightly larger than that at T_2 but not as large as at T_1. Finally, when E is held constant, the temperature is returned to its initial value by simultaneously adding charge and transferring heat.

A typical electric circuit for executing this cycle is shown in figure 1(b). The capacitor is initially charged through the diode by the battery to state 1. With both the diode and the silicon control rectifier (an electronic switch that can be triggered on but not off (ref. 7)) blocking current flow, the voltage on the capacitor is increased by changing the temperature from T_1 to T_2, thereby reducing ϵ. The silicon control rectifier is then triggered, which allows the capacitor to discharge through the load and the battery (state 2 to state 3). Proper choice of load size will allow the battery to receive exactly the energy it initially delivered. Finally, the capacitor is returned to its initial state with the battery again providing the required charge.

Cycle B. - The first process is the same as in cycle A; that is, at constant charge the field is increased to E_2 while the temperature changes to T_2. Electric energy is then removed (delivered to the load) adiabatically (and isentropically); this condition decreases the field to E_3 and changes the temperature to T_3. At constant charge heat is transferred, and therefore, the temperature is changed to T_4 so that ϵ increases, and the field drops to E_4. Finally, the capacitor is charged adiabatically (and isentropically) and is returned to the initial electric field and temperature.

A typical circuit for executing cycle B is presented in figure 1(c). During the first process, current is not allowed to flow from the capacitor, which allows voltage to be increased at constant charge. Next the bistable switching circuit (flip-flop) is triggered on, which allows the capacitor to discharge through the load and the battery; the inductor can be selected so that the battery receives exactly the same energy it initially delivered. When the field has dropped to E_3, the flip-flop is triggered off, the capacitor is therefore isolated from the load and the battery, and the second constant charge process is allowed to take place. When the field has dropped to E_4, the silicon control rectifier is triggered and the battery is allowed to charge the capacitor back to its initial state.

These circuits are given as an aid to understanding the cycles and should not be considered the best available. Further details of electric circuitry

and physical construction are purposely avoided in this analysis. Another (less efficient) thermodynamic cycle and a variety of possible circuits can be found in references 8 and 9. Other possible cycles have been omitted on the grounds of lower efficiency or of impracticality.

Mathematical Description of Cycles

The processes making up the two cycles discussed can be analyzed in terms of the thermodynamic parameters of internal energy U and entropy S of the dielectric. When performing this analysis the following relations are needed: the first law of thermodynamics,

$$dU = dQ + dW \tag{7}$$

where Q is the thermal energy; the definition of entropy,

$$dS = \frac{dQ}{T} \tag{8}$$

and an expression for dW, the electrical energy added, in terms of appropriate independent variables and the properties of the dielectric material.

If the electric field E can be expressed as a univalent function of the electric displacement D and if the dielectric is an isotropic medium, then the electric energy density is given by (ref. 10)

$$dW = E\, dD \tag{9a}$$

leading to the expression

$$W = \int E(D)\, dD \tag{9b}$$

(all quantities are expressed in rationalized mks units).

When the previous expressions are used, the processes making up the two cycles discussed can be analyzed. In integrated form, the first law of thermodynamics becomes

$$\Delta U = \int_a^b dQ + \int_a^b E\, dD \tag{10}$$

where both integrals are line integrals.

In a constant-charge process, there will be no electrical energy transferred; hence, the second integral in equation (10) is zero. This is true for a parallel plate capacitor, since the electric displacement D is numerically equal to the charge density. The heat transferred in this process can then be obtained from the end point values of U

$$\int_a^b dQ = U(T_b,E_b) - U(T_a,E_a) \tag{11a}$$

with the condition that

$$D(T_b,E_b) = D(T_a,E_a) \tag{11b}$$

For an isentropic process, the electrical energy transferred is given by

$$\int_a^b E\, dD = U(T_b,E_b) - U(T_a,E_a) \tag{12a}$$

with the condition

$$S(T_b,E_b) = S(T_a,E_a) \tag{12b}$$

This adiabatic (and isentropic) process can be achieved in practice by simply charging or discharging a capacitor rapidly (assuming a lossless dielectric). Such a process must result in a change in temperture for a dielectric whose permittivity varies with temperature if equation (12b) is to be satisfied. Intuitively it would be expected that such a temperature change would be small. This effect has been measured (ref. 11), for a material whose dielectric constant changes very rapidly with temperature, at fields up to 0.75×10^6 volts per meter. The maximum temperature change recorded was about 0.5° K. This small change in temperature corresponds to a very large change in electric field and is important in the calculation of work and efficiency; hence, it cannot be ignored in the analysis.

In a constant-field process, the electrical energy transferred can be calculated directly since

$$\int_a^b E\, dD = E\left[D(T_b,E) - D(T_a,E)\right] \tag{13a}$$

$$\int_a^b dQ = U(T_b,E) - U(T_a,E) - E\left[D(T_b,E) - D(T_a,E)\right] \tag{13b}$$

The condition demanded by the process is

$$E = E_a = E_b = \text{constant} \tag{13c}$$

Explicit expressions for U and S are derived in appendix B.

Equations (11) and (13) can be used to calculate the thermal efficiency for both cycles with the usual definition, $\eta = \dfrac{\text{heat in - heat out}}{\text{heat in}}$. This is

done explicitly in appendix C.

When putting these processes together to form a cycle, it is necessary to choose a set of end point variables. Each end point is specified by a field and a temperature. Each process gives one equation relating two end points (four variables). Cycle A, which consists of three processes, is specified by three end points (six variables). The processes furnish three equations relating the six variables; hence, only three variables may be chosen arbitrarily. By the same argument it can be shown that four variables must be chosen arbitrarily to specify cycle B.

The basic criterion used for deciding which variables to specify was ease of interpretation. The variables specified for cycle A were maximum temperature, minimum temperature, and maximum electric field E_2. This choice of temperatures facilitates comparison of cycle efficiency with Carnot efficiency while the maximum electric field is limited by the breakdown strength of the particular dielectric used. For cycle B the same three variables were specified, with the addition of the field E_3 remaining in the dielectric after power has been delivered to the load. The ratio of this field to the maximum field E_3/E_2 gives a qualitative indication of how much energy remains in the capacitor after power has been delivered to the load.

Internal Energy and Entropy

In developing expressions for internal energy and entropy, equations (7), (8), and (9) are needed. All calculations that follow are subject to the assumption of a parallel plate capacitor in which edge effects are neglected. This assumption reduces the problem to a one-dimensional form.

The dielectric properties of some materials, such as ferroelectrics (ref. 12), depend on both temperature and electric field. This relation between dielectric constant, temperature, and field can be expressed in any one of the following ways:

$$\epsilon = \epsilon(T,E) \tag{14a}$$

or

$$D = D[\epsilon(T),E] \tag{14b}$$

where $\epsilon(T)$ describes the behavior of the dielectric at zero field, or

$$D = \epsilon_o E + P(E,T) \tag{14c}$$

where P is the polarization of the dielectric. For the purposes of this report, expression (14b) is used since it is a convenient form for a class of materials of interest. In this case T and E are taken as the independent variables, which gives

$$dD = \frac{\partial D}{\partial \epsilon} \frac{d\epsilon}{dT} dT + \frac{\partial D}{\partial E} dE \tag{15}$$

From equations (14) and (15) it is possible to derive the following equations for S and U (appendix B):

$$U = \rho c T + \int E \frac{\partial D}{\partial E} dE + T \int \frac{d\epsilon}{dT} \frac{\partial D}{\partial \epsilon} dE \tag{16a}$$

$$S = \rho c \ln T + \int \frac{d\epsilon}{dT} \frac{\partial D}{\partial \epsilon} dE \tag{16b}$$

For materials such as polyethylene terepthalate, the dielectric constant is a function only of temperature; hence,

$$\epsilon = \epsilon(T) \tag{17a}$$

and

$$D = \epsilon_o \epsilon(T) E \tag{17b}$$

The functions S and U can be calculated by simply substituting these expressions into equations (16), which yields

$$U = \rho c T + \frac{\epsilon_o E^2}{2} \left[\epsilon(T) + T \frac{d\epsilon}{dT} \right] \tag{17c}$$

$$S = \rho c \ln T + \frac{\epsilon_o E^2}{2} \frac{d\epsilon}{dT} \tag{17d}$$

Choice of Specific Materials

The basic criteria for selecting specific materials for detailed study are the following: First, the dielectric constant must vary with temperature, the more rapidly the better; and second, the material must be able to store a large amount of electric energy per unit volume. The second criterion can be interpreted with the help of the expression

$$W = \frac{1}{2} \epsilon_o \epsilon E^2 \tag{18}$$

which is an approximation to the exact expression given in equation (9b). This shows that the second criterion demands high dielectric constant and/or the ability to support high electric fields.

On the basis of these criteria two materials, polyethelene terephthalate and barium titanate ($BaTiO_3$), were selected for detailed study. The temperature dependence of the dielectric constants of these materials is shown in figures 3(a) and 3(b), which were taken from references 12 to 14. (The hyster-

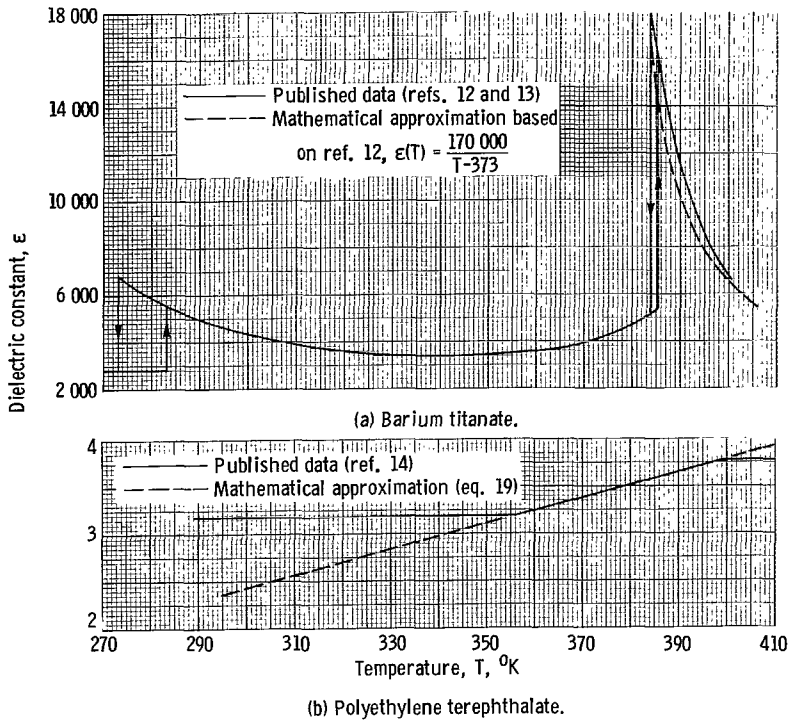

Figure 3. - Temperature dependence of dielectric constants of two materials of interest for generator.

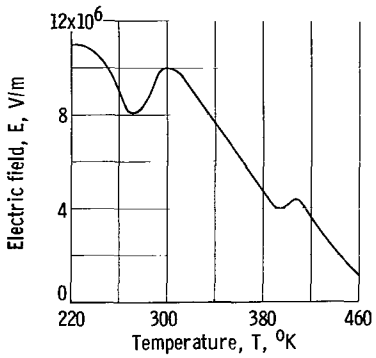

Figure 4. - Temperature dependence of breakdown field for barium titanate (ref. 17). Specimen thickness, 0.1 centimeter.

esis for barium titanate shown in fig. 3(a) will be discussed later.) In addition to the temperature variation, reference 15 shows that for barium titanate the dielectric constant decreases rapidly with increasing electric field. The maximum electric fields that can be supported are about 5×10^8 volts per meter for polyethylene terephthalate (ref. 16) and about 10^7 volts per meter for barium titanate. The actual breakdown voltage for barium titanate is a function of temperature (ref. 17). Figure 4 shows typical data from this reference. The figure of 10^7 volts per meter is an upper limit.

The use of typical values of ϵ from figure 3 (viz., 3.5 for polyethylene terephthalate and 10 000 for barium titanate) and the previous breakdown data in equation (18) indicates that both materials are capable of storing approximately 4 joules per cubic centimeter, which is about the highest that can be achieved with solid dielectrics (refs. 18 and 19). When data from figure 3 are used in equations (5) and (6) and when both materials are assumed to give the same initial energy density, it can be estimated that barium titanate should deliver 5 to 10 times more energy per unit volume than polyethylene terephthalate for a given temperature range due to the very rapid variation of its dielectric constant with temperature; barium titanate would therefore lead to the generator with the better thermal efficiency.

Mathematical Description of the Materials

In order to use equations (11), (12), (13), and (16) to analyze this gen-

erator, it is helpful to have a simple mathematical description of the properties of the previous materials in the form of either equation (14a) or (14b). In view of the assumptions used in the derivation of equations (16) and (17), it is necessary that the functions selected be twice differentiable; this explicitly rules out discontinuities such as would be suggested by figure 3(a). Since the purpose of this report is to find the upper limits on the capabilities of a power conversion device, as well as to show the effects of the appropriate parameters on its performance, the mathematical approximations have been chosen so as to produce optimistic results whenever an exact fit to the data is not possible. This requires that the functions selected predict a more rapid variation of dielectric constant with temperature and/or a greater magnitude of dielectric constant than is actually shown in the data.

Polyethylene terephthalate. - The data in figure 3(b) are very nearly linear over a range of temperatures; hence, the mathematical approximation chosen was a linear extrapolation:

$$\epsilon(T) = \alpha + \beta T \tag{19}$$

where

$$\alpha = -1.6$$

$$\beta = 0.0135^{\circ}\ K^{-1}$$

and T is expressed in $^{\circ}K$. This provides an accurate curve fit at temperatures between 355° and 400° K.

Barium titanate. - From the data presented in figure 3(a), it is clear that a simple mathematical function cannot be found that will describe barium titanate over the entire temperature range presented. Additional difficulties in finding a simple mathematical description are introduced by three properties of barium titanate. First, in the temperature range between 275° and 395° K, barium titanate exhibits a spontaneous polarization (ref. 12). The polarization varies with applied field E in the same manner as does magnetic induction with magnetic intensity for soft iron (refs. 12, 13, and 20); that is, the variables are related by a hysteresis loop which cannot be described by a univalent function as required in the derivation of equations (16), (17c), and (17d). Second, single crystals of barium titanate exhibit an abrupt change in dielectric constant (fig. 3(a)) at about 385° K (referred to as the "Curie temperature" in the literature), which corresponds to a sudden change in crystal structure (ref. 12). The exact temperature at which this transition occurs depends on the direction of approach to the critical region (ref. 21); this is indicated by arrows in figure 3(a). In addition, the Curie temperature is shifted upward by the application of an electric field (refs. 22 and 23). Finally, the properties of a single crystal of barium titanate are strongly anisotropic (ref. 12); the dielectric constant changes by more than an order of magnitude as crystal orientation is changed.

In order to keep the calculation optimistic, an approximation based on the properties of a single crystal must use the properties associated with the

"best" orientation of the crystal; namely, the orientation that results in the highest dielectric constant.

In order to avoid the spontaneous polarization and resulting hysteresis loops, it is desirable to limit the mathematical description to the range of temperatures above the Curie temperature. An analysis of a power conversion device using barium titanate in the region of the Curie temperature has been published (ref. 24) in which an attempt has been made to include the discontinuity of the dielectric constant and the dependence of the Curie temperature on applied field as described in reference 23. The resulting expressions, which involve a unit step function, are considered too unwieldy to be of use in this analysis.

In polycrystalline (ceramic) form, barium titanate does not exhibit the discontinuity and the temperature hysteresis apparent in figure 3(a) and discussed in reference 25. The dielectric constant is much smaller than for a single crystal and would result in lower performance. A theory has been published that predicts the behavior of such ceramics (ref. 26); however, it involves a statistical analysis that is not readily adaptable to this calculation.

A phenomenological theory has been proposed (ref. 27) that predicts the behavior of single crystals of barium titanate over the entire temperature range shown in figure 3(a). This theory consists of a power series expansion for the thermodynamic free energy function in terms of the polarization P. For materials with high dielectric constant, P is approximately equal to D. This can be shown by examining the equation

$$D = \epsilon_o E + P(E,T) = \epsilon_o \epsilon(T,E) E$$

If $\epsilon \gg \epsilon_o$, the term $\epsilon_o E$ becomes negligible and $P \approx D$. In general form this power series is too complex to be useful in this analysis; however, it is shown in reference 28 that above the Curie temperature the equation can be simplified and rewritten in the form

$$E = \frac{D}{\epsilon_o \epsilon(T)} + \gamma D^3 \tag{20a}$$

where

$$\epsilon(T) = \frac{p}{T - T_o} \tag{20b}$$

$$D = D[\epsilon(T), E]$$

if the P^5 (and therefore the D^5) term is neglected.

Equation 20(a), which was also obtained by fitting of experimental data in reference 15 prior to the development of the theory of reference 28, was selected to describe barium titanate in the present report. Specific values of

p and T_o (the so-called characteristic temperature) were taken from reference 12:

$$p = 170\ 000$$

$$T_o = 373^\circ\ K$$

Under the condition of low electric field, the γD^3 term of equation (20a) becomes negligible and the equation can be rewritten in the form of equation (17b); hence, equation (20b) adequately describes the dielectric in this situation. Equation (20b) is plotted on figure 3(a) (dashed curve); it very nearly coincides with the data (taken at low applied field) in the region above the Curie temperature. For higher fields, equation (20a) must be used. Equation (20a) has been used in the analysis of a power conversion device (ref. 29) by using a linear dependence of γ on temperature (as was shown to be approximately valid in ref. 28). The resulting expressions become unwieldy if applied to the thermodynamic cycles of interest in this report. According to reference 28, γ varies by about a factor of two over a temperature range of 30° K, a range of interest in the analysis. Published data (refs. 28 and 15) give typical values of γ for different samples of the same material (barium titanate) ranging all the way from 5×10^9 to 5×10^{11} (rationalized mks units). Since the variation in the published data is two orders of magnitude, while the temperature variation is only a factor of two, it was considered pointless to attempt to include the temperature effect. The approach taken was to consider γ a constant and determine the effect of different (constant) values of this parameter.

Some Properties of Final Equations

The final equations describing the two cycles for both materials are obtained by substituting equations (19) and (20) into equations (16) and (17), which are in turn used in equations (11) to (13). Some details of this process are given in appendix C.

From the forms of some of the final equations, obtained by substituting the explicit expression for U and S for a given dielectric material (eqs. (C10), (C11), (C13), and (C14)), it is possible to obtain a qualitative idea of the performance of these cycles. An examination of these equations allows determination of limitations on electric field other than breakdown, of some relations among the endpoint variables, and of the maximum thermal efficiency for both cycles.

Limitations on electric field. - For both cycles, the first process requires conversion of thermal energy to electrical energy at constant charge, which requires that $\epsilon(T_2) < \epsilon(T_1)$, as indicated by equations (5) and (6). This means that for polyethylene terephthalate $T_2 < T_1$; therefore, heat must be rejected during the process. For barium titanate (described by eq. (20)) it is necessary that $T_2 > T_1$, which requires that heat be added. Limitations on electric field that might be imposed by the conditions can be checked by examining the equation

$$\int_1^2 dQ = \rho c(T_2 - T_1) - \frac{\epsilon_o E_2^2}{2}\left\{\left[\frac{\epsilon(T_2)}{\epsilon(T_1)}\right]^2\left[\epsilon(T_1) + T_1\left(\frac{d\epsilon}{dT}\right)_{T_1}\right] - \left[\epsilon(T_2) + T\left(\frac{d\epsilon}{dT}\right)_{T_2}\right]\right\} \tag{21}$$

which results from equations (11), (14b), and (17a).

When equation (19) is used for polyethylene terephthalate, equation (21) reduces to

$$\int_1^2 dQ = \rho c(T_2 - T_1) + \frac{\epsilon_o E_2^2}{2}\left\{\frac{\beta^2(T_1 - T_2)\left[\alpha(T_1 + T_2) + 2\beta T_1 T_2\right]}{(\alpha + \beta T_1)^2}\right\} < 0$$

This sets the following upper limit on E_2:

$$\left(E_2^2\right) < \frac{2\rho c(\alpha + \beta T_1)^2}{\epsilon_o \beta^2\left[\alpha(T_1 + T_2) + 2\beta T_1 T_2\right]} = \left(E_2^2\right)_{max}$$

If E_2 is greater than this value, the energy output will be negative; that is, the thermodynamic cycle will become a refrigeration cycle. Using numbers appropriate to polyethylene terephthalate (appendix C) gives a limit on E of about 3×10^9 volts per meter ($T_1 = 400^\circ$ K, $T_2 = 350^\circ$ K). Since the net electrical energy generated will be zero for $E_2 = 0$ and also for the maximum allowable value of E_2 (as calculated), there will be some value of E_2 between these extremes that will yield a maximum energy output per cycle. This was calculated and found to be about 2×10^9 volts per meter for the same T_1 and T_2 used previously. Since these values are 5 to 10 times the breakdown field for polyethylene terephthalate, the limitation on E_2 will be the breakdown field rather than the field at which the energy output goes to zero.

For barium titanate, described by equation (20b), equation (21) reduces to

$$\int_1^2 dQ = \rho c(T_2 - T_1) > 0$$

which demands only that $T_2 > T_1$. There is no dependence on E (terms including E_2 cancel out of the expression); hence, there is no upper limit on its magnitude other than breakdown.

Relation among endpoint variables. - For both cycles the second (isentropic) process must result in energy output; that is, $\int_2^3 dW < 0$. By argu-

ments similar to those used previously, it can be shown that this requirement, the condition on the first process, and the nature of the cycles lead to the following relations among the endpoint temperatures:

Polyethlene terephthalate:

$$\text{Cycle A:} \quad T_1 > T_3 > T_2$$

$$\text{Cycle B:} \quad T_4 > T_1 > T_2$$

$$T_4 > T_3 > T_2$$

Barium Titanate:

$$\text{Cycle A:} \quad T_2 > T_3 > T_1$$

$$\text{Cycle B:} \quad T_2 > T_1 > T_4$$

$$T_2 > T_3 > T_4$$

The field relations are the same for both materials:

$$\text{Cycle A:} \quad E_2 > E_3 = E_1$$

$$\text{Cycle B:} \quad E_2 > E_3 > E_4$$

$$E_2 > E_1 > E_4$$

Maximum theoretical efficiency. - It is possible to find the maximum theoretical efficiency of cycle A by using the approximate relation for barium titanate given by equation (20b). Using this expression for ϵ in equations (11), (12), (13), and (17) leads to the expression

$$\eta = \frac{T_2 - T_3 - \dfrac{(2T_1 - T_o)T_3 - T_oT_1}{T_1 + T_3 - 2T_o} \ln \dfrac{T_2}{T_3}}{T_2 - T_1} \tag{22}$$

where T_3 is obtained from

$$E_2^2 = \frac{2\rho c}{\epsilon_o p} \frac{(T_2 - T_o)^2}{1 - \left(\dfrac{T_1 - T_o}{T_3 - T_o}\right)^2} \ln \frac{T_2}{T_3} \tag{23}$$

which comes from equations (11b), (12d), and (13c). From equation (23) it can

be seen that $T_3 = T_1$ gives an infinite E_2, which can be shown to give maximum efficiency for this material. Making the substitution $T_3 = T_1$ in equation (22) yields

$$\eta_{max} = 1 - \frac{T_1}{T_2 - T_1} \ln \frac{T_2}{T_1}$$

For $T_2 - T_1 \ll T_1$ this reduces to

$$\eta_{max} \approx \frac{1}{2} \frac{T_2 - T_1}{T_1}$$

The Carnot efficiency is given by

$$\eta_{Carnot} = \frac{T_2 - T_1}{T_2}$$

Hence,

$$\frac{\eta_{max}}{\eta_{Carnot}} \approx \frac{1}{2} \frac{T_2}{T_1} \approx \frac{1}{2} \qquad \text{for} \quad \frac{T_2}{T_1} \approx 1$$

It is possible to find the maximum theoretical efficiency of cycle B by using the approximate description of barium titanate given by equation (20b). The use of this expression for ϵ in equations (17a), (11a), (C14), and the definition of efficiency leads to the result

$$\eta = 1 - \frac{T_3 - T_4}{T_2 - T_1}$$

Further manipulation of equations (C14) yields the relation

$$\frac{T_2}{T_3} = \frac{T_1}{T_4} \tag{24}$$

Therefore,

$$\eta = \frac{T_2 - T_3}{T_2} \tag{25}$$

Carnot efficiency is given by the expression

$$\eta_{Carnot} = \frac{T_2 - T_4}{T_2}$$

since

$$T_2 = T_{max}$$

$$T_4 = T_{min}$$

The limiting condition that must occur in order to yield maximum theoretical efficiency for cycle B is that the net energy output approach zero. This equation can be written explicitly by using equations (C2a), (C13), and (C14) noting that

$$W = 0 = \Delta Q_{1-2} + \Delta Q_{3-4} = \Delta W_{2-3} + \Delta W_{4-1}$$

This equation simplifies to the relation

$$T_2 - T_1 + T_4 - T_3 = 0 \tag{26}$$

Solution of this equation with equation (24) leads to the relations

$$T_3 = T_4 \tag{27a}$$

$$T_2 = T_1 \tag{27b}$$

Consequently, the expression for efficiency (eq. (25)) reduces to

$$\eta = \frac{T_2 - T_4}{T_2}$$

which is equal to the Carnot efficiency.

The relations among the other parameters demanded by this maximum efficiency condition can be found by using equations (27), (C2a), and (C2b) with equations (C14). The results of this calculation are as follows:

$$E_1 = E_2$$

$$E_3 = E_4$$

$$\frac{2\rho c}{\epsilon_o p} \ln \frac{T_2}{T_4} = \frac{E_2^2}{(T_2 - T_o)^2} - \frac{E_4^2}{(T_4 - T_o)^2} \tag{28}$$

It can be seen that there is no requirement of infinite fields as was the case for cycle A.

From the previous calculations it is apparent that the best possible per-

TABLE I. - TYPICAL PERFORMANCE DATA

Figure	Thermal efficiency, η, percent	Electric energy output, W, J/cu m	Maximum electric field strength, E_{max}, V/m	Discharge fraction, E_3/E_2	Correction coefficient, γ, $(V)(m^5)/C^3$
5(a)	0.0704	0.0501×10^{-6}	3.43×10^8	----	-
5(b)	.1276	.090	3.43×10^8	0.83	-
5(c)	.48	.17	7.22×10^6	----	0
5(d)	.78	.213	7.22×10^6	.60	0

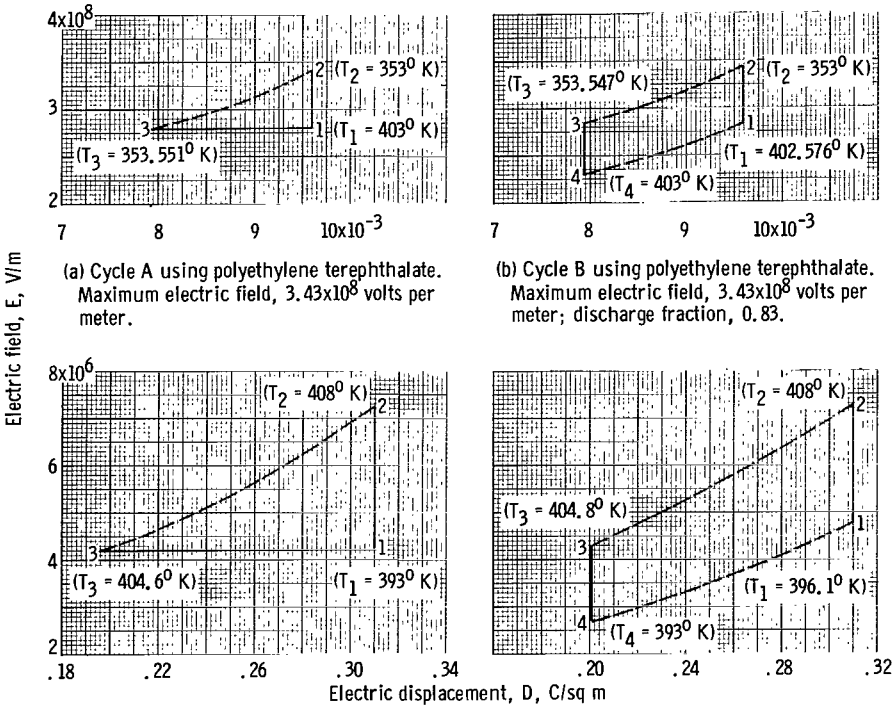

(a) Cycle A using polyethylene terephthalate. Maximum electric field, 3.43×10^8 volts per meter.

(b) Cycle B using polyethylene terephthalate. Maximum electric field, 3.43×10^8 volts per meter; discharge fraction, 0.83.

(c) Cycle A using barium titanate. Maximum electric field, 7.22×10^6 volts per meter; correction coefficient, 0.

(d) Cycle B using barium titanate. Maximum electric field, 7.22×10^6 volts per meter; discharge fraction, 0.6; correction coefficient, 0.

Figure 5. - Typical examples of both thermodynamic cycles with both materials.

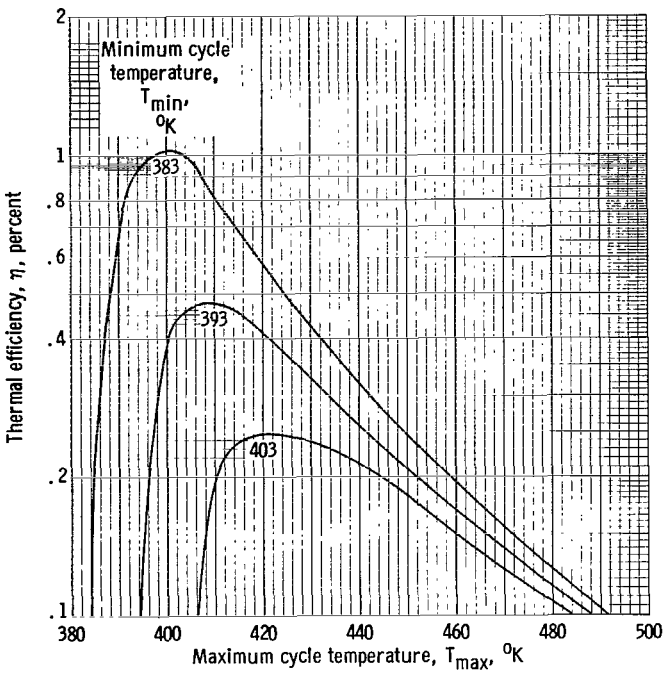

Figure 6. - Typical efficiency curves for cycle A with barium titanate. Maximum electric field, 7.22×10^6 volts per meter; correction coefficient, 0.

formance for this generator can be obtained from cycle B by using barium titanate as the dielectric.

RESULTS AND DISCUSSION

With the preceding theory and approximations, a numerical analysis was performed with an IBM 7094 computer. The systems of equations (C11) and (C14) were solved by the Newton-Raphson method (ref. 30), and the results were then used in the sets of equations (C10) and (C13). A thermodynamic analysis was done for cycles A and B by using polyethylene terephthalate and barium titanate. Typical numerical results for each cycle are summarized in table I and figure 5 (the adiabatic processes are shown as dashed curves since their exact shape was not calculated).

The heat-transfer equations were then written for the rotating cylinder (fig. 1(a), p. 2) in space, heated by the sun and by a nuclear reactor, and solved numerically (appendix D). When the results of the thermodynamic analysis and the heat-transfer calculation were combined with the help of a suitable temperature scaling technique (discussed later), it was possible to determine the best (lowest) specific weights that could reasonably be expected for the dielectric material in this type of generator.

Thermodynamic Calculations

Cycle A. - The performance of cycle A using barium titanate (as approximated by eq. (20a)) is shown in figures 6 to 10. The curves in figure 6 exhibit maxima which indicate that for any combination of the parameters there is some optimum value of $T_{max} - T_{min}$ that yields best efficiency. Figure 7 shows the magnitude of these maxima as functions of the parameters T_{min}, E_{max}, and γ, while figure 8 locates the values of T_{max} required to yield these maxima. It can be seen that the best efficiencies attainable with a realistic value of E_{max} (7×10^6 V/m) are in the neighborhood of 1.0 percent, while realistic values of T_{min} and γ (393° K and 10^9 (V)$(m^5)/C^3$, respectively) reduce this to about 0.1 percent. The maximum theoretical efficiencies (half the Carnot efficiency) corresponding to these values are 1.9 and 6.4 percent, respectively.

The energy output curves for barium titanate have the same form as the

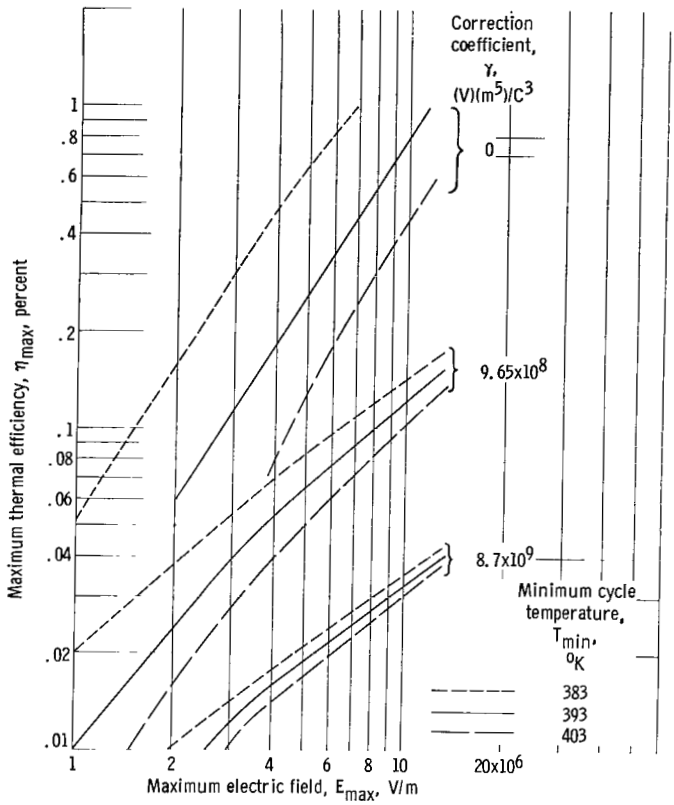

Figure 7. - Maximum thermal efficiency as function of maximum electric field for cycle A using barium titanate.

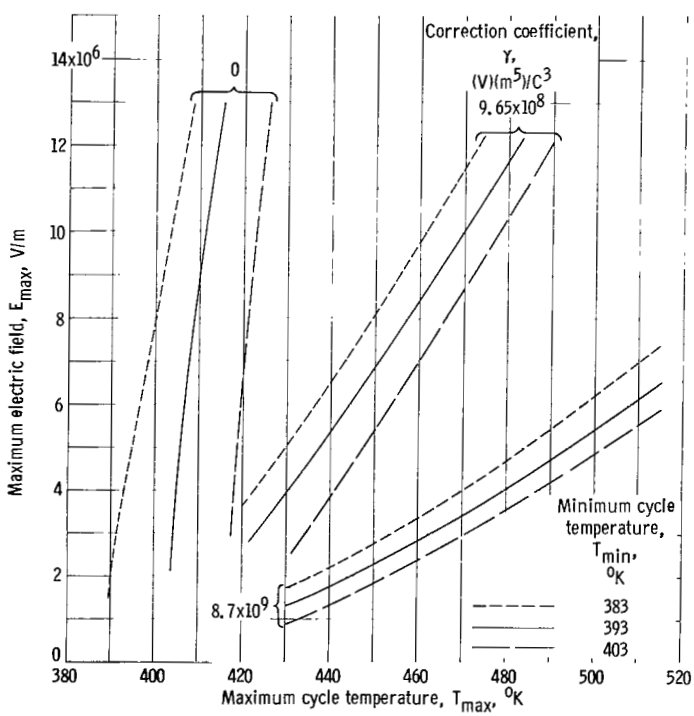

Figure 8. - Maximum cycle temperature required to yield maximum thermal efficiency for barium titanate using cycle A.

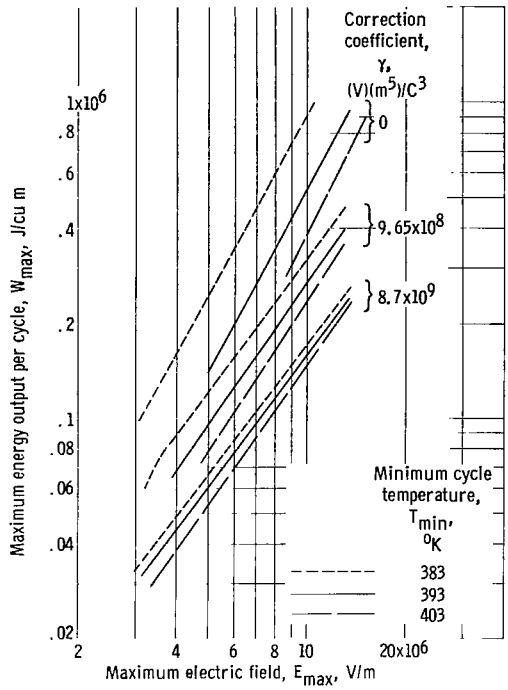

Figure 9. - Maximum energy output per cycle per unit volume. Cycle A, barium titanate.

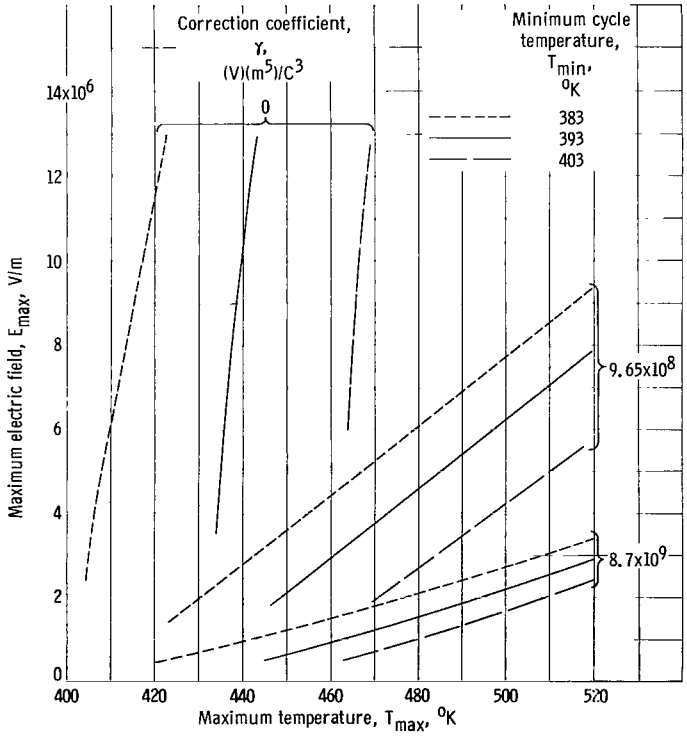

Figure 10. - Maximum cycle temperature required to yield maximum energy output for cycle A using barium titanate.

efficiency curves (fig. 6). Figures 9 and 10 give the locations and magnitudes of the maxima and therefore are similar to figures 7 and 8. It can be seen that the best energy output available with a realistic value of E_{max} (7×10^6 V/m) is 0.45×10^6 joules per cubic meter per cycle, while inclusion of realistic values of T_{min} and γ (393° K and 10^9 (V)$(m^5)/C^3$, respectively) reduces this to 0.16×10^6 joules per cubic meter per cycle.

Cycle A was also analyzed using polyethylene terephthalate as approximated by equation (19). The results of this calculation can be summarized by comparing figures 5(a) and 5(c) (see p. 18) and examining the performance data (table I) for these cases:

(1) Thermal efficiency, η, 0.0704 percent; electric energy output, W, 0.0501×10^6 joules per cubic meter per cycle (fig. 5(a))

(2) Thermal efficiency, η, 0.48 percent; electric energy output, W, 0.17×10^6 joules per cubic meter per cycle (fig. 5(c))

As can be seen, both efficiency and energy output are considerably lower for polyethylene terephthalate than for barium titanate. Consequently, a more detailed discussion of this combination is not of interest.

Cycle B. - The performance of cycle B using barium titanate is presented in figures 11 and 12. An examination of figure (11) shows three general features of interest. First, as the temperature difference $T_{max} - T_{min}$ decreases, the thermal efficiency increases toward Carnot efficiency. Second, efficiency has a parabolic dependence on the discharge fraction, the maximum occurring for $E_3/E_2 = 0$. Third, to a good approximation, efficiency varies directly as the square of the parameter E_{max}. From this set of curves it can be seen that by using a reasonable E_{max} (7.22×10^6 V/m), a reasonable value for E_3/E_2 (0.2), and a value of T_{min} (393° K), one could expect up to 1.7-percent thermal efficiency (very nearly Carnot efficiency for the value of T_{max} (403° K) selected). If it is assumed that γ has roughly the same effect on this cycle as it had on cycle A (fig. 7), inclusion of a realistic value (10^9) would reduce the expected efficiency by a factor of 5 to 0.34 percent. This performance is about three times better than that of cycle A.

The energy output curves are shown in figure 12. As can be seen from figures 12(a) and 12(b), these curves exhibit maxima, indicating an optimum value for the parameter T_{max}, and pass through zero at a value of T_{max} corresponding to Carnot efficiency (fig. 11(a)). Figures 12(c) and 12(d) show that the net energy output varies with the parameters E_3/E_2 and E_{max} in the same way as do the efficiency curves. This set of curves shows that for the same values of E_{max}, E_3/E_2, and T_{min} used in the efficiency discussion, one would expect an energy output as high as 0.4×10^6 joules per cubic meter per cycle. If it is assumed that γ affects this cycle as it did cycle A (fig. 9), inclusion of a realistic value (10^9) would reduce the expected energy output by a factor of 2 to 0.2×10^6 joules per cubic meter per cycle.

Cycle B was also analyzed using polyethylene terephthalate as approximated by equation (19). The results of this calculation can be summarized by com-

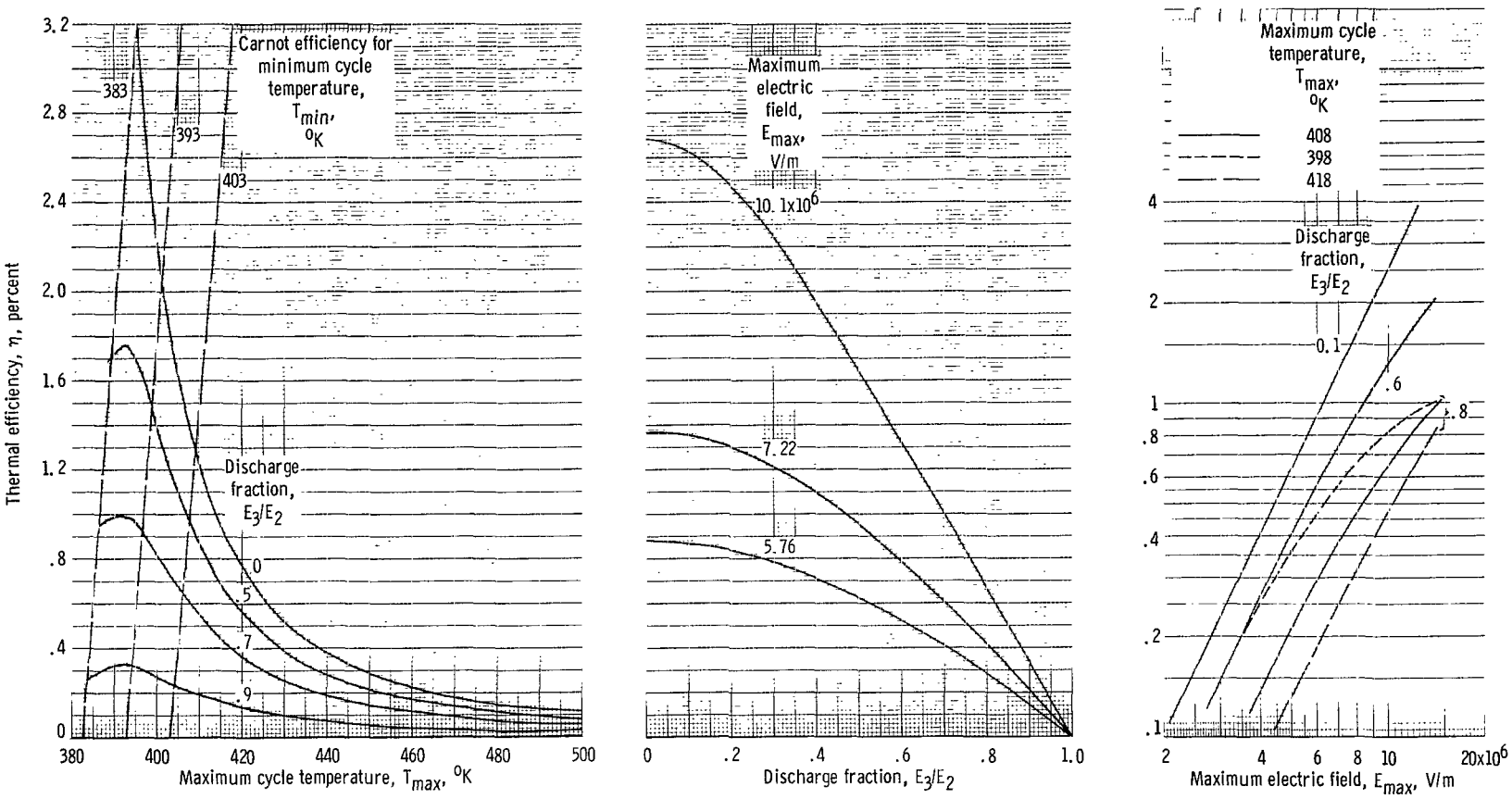

(a) Maximum electric field, 7.22×10^6 volts per meter; correction coefficient, 0.

(b) Minimum cycle temperature, 393° K; maximum cycle temperature, 408° K; correction coefficient, 0.

(c) Minimum cycle temperature, 393° K.

Figure 11. - Efficiency curves for cycle B with barium titanate.

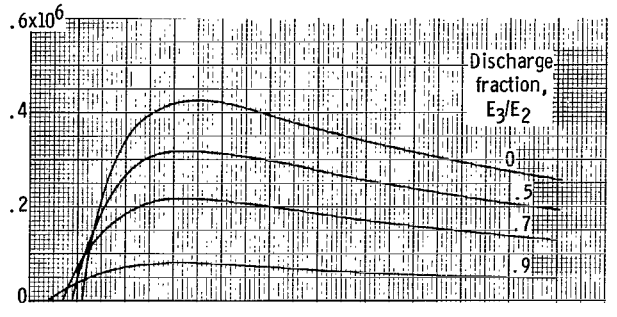

(a) Minimum cycle temperature, 393° K; maximum electric field, 7.22×10^6 volts per meter; correction coefficient, 0.

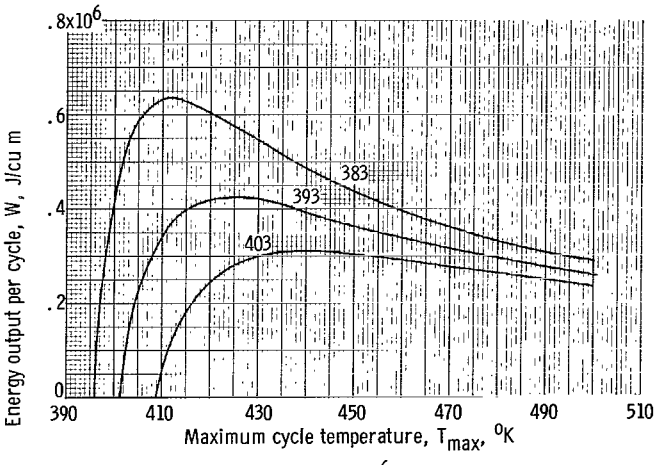

(b) Maximum electric field, 7.22×10^6 volts per meter; discharge fraction, 0; correction coefficient, 0.

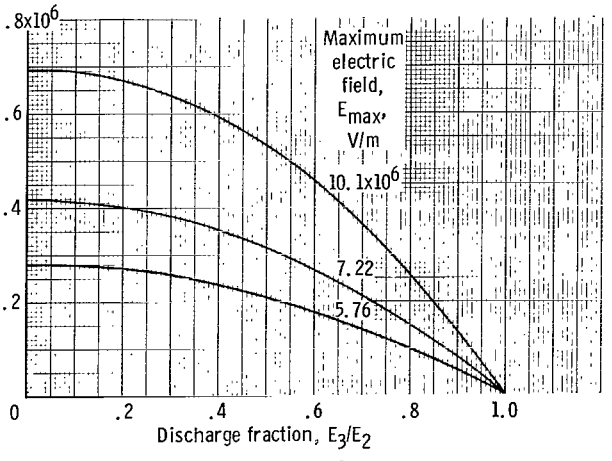

(c) Minimum cycle temperature, 393° K; maximum cycle temperature, 418° K; correction coefficient, 0.

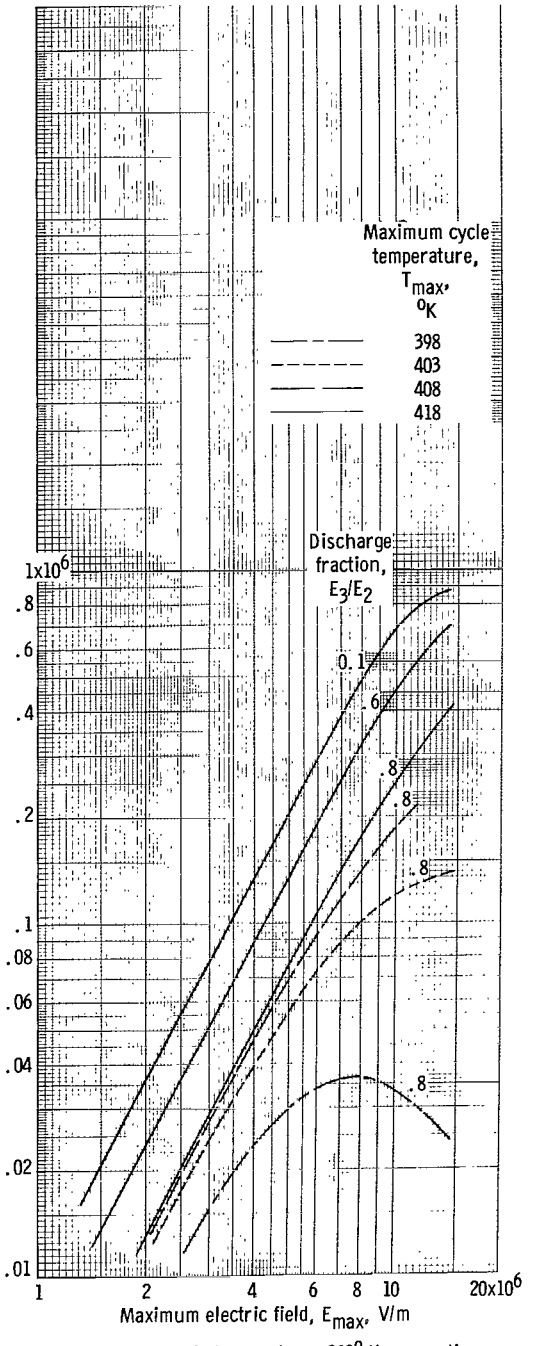

(d) Minimum cycle temperature, 393° K; correction coefficient, 0.

Figure 12. - Energy output, curves for cycle B with barium titanate.

paring figures 5(b) and 5(d) and examining the performance data (table I) for these cases:

(1) Thermal efficiency, η, 0.1276 percent; electric energy output, W, 0.090×10^6 joules per cubic meter per cycle (fig. 5(b))

(2) Thermal efficiency, η, 0.78 percent; electric energy output, W, 0.213×10^6 joules per cubic meter per cycle (fig. 5(d))

As can be seen, both efficiency and energy output are considerably lower for polyethylene terephthalate than for barium titanate. Consequently, a more detailed discussion of this combination is not of interest.

Best performance. - From the preceding discussion and figures it is clear that barium titanate is the more promising of the two dielectrics considered. When this material is used, cycle B is two to three times as efficient as cycle A and yields roughly the same energy output per cycle. A comparison of figures 5(c) and 5(d) and the attached performance data provides a numerical example of this trend. Since the goal of this study is to achieve maximum power output with minimum weight, the combination of barium titanate and cycle B is the only one considered in subsequent specific weight calculations.

Heat-Transfer Calculations

In order to find the specific weight of this system, it is necessary to find the number of cycles executed per second and the corresponding maximum and minimum temperatures, which in turn give the energy output per unit volume per cycle from the thermodynamic analysis. Specific weight is then given explicitly by the expression ρ/Wf. This is accomplished by solving the heat-transfer equations (appendix D) for the design of figure 1(a) and using the results (maximum and minimum temperatures) with the thermodynamic data (viz., the energy output per unit volume curves).

Typical temperature distributions on a cylinder rotating in space close to the Earth and heated by the sun were obtained from equation (D1) and are presented in figure 13. The "rotation parameter" λ is given by

$$\lambda = \frac{\sigma \delta_2}{2\pi f L \rho c} \tag{29}$$

as in reference 2. Taking the special case of surface emissivity ($\delta_2 = 1$) with ρ and c taken at values appropriate to barium titanate (appendix C) and expressing L in meters lead to

$$\lambda = 3.95 \times 10^{-11} (fL)^{-1}$$

The effect on the temperature distribution of executing cycle A with a hypothetical material having dielectric properties similar to those of barium titanate (scaled to fit the temperature range encountered) was calculated for

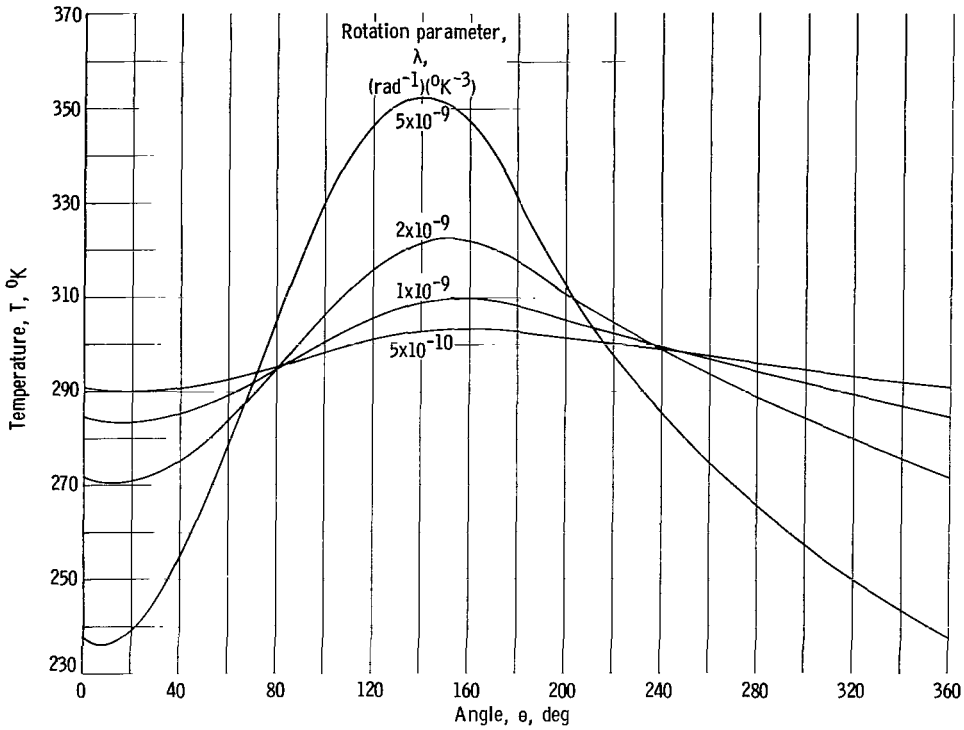

Figure 13. - Temperature distribution for thin-walled hollow cylinder in vicinity of Earth. Incident power, 1390 watts per square meter.

a range of the parameters λ and $T_{min} - T_o$ (appendix D). The solution shown in figure 14 represents a case in which the effect on the temperature distribution is a maximum. Since all thermodynamic calculations were done with T_{max} and T_{min} as parameters, figure 14 shows that the effects of the thermodynamic cycle on the temperature distribution may be neglected and the results for the "inert cylinder" used. This conclusion is also valid for cycle B, because the only effect of cycle B would be to introduce a second discontinuity into the temperature distribution (from T_{min} to $T_{min} + 2^{o}$ or 3^{o} K).

Since lighter weight can result from higher operating temperatures, the possibility of heating the generator with a nuclear reactor was considered. When figure 18 and the equations in appendix D were used, temperature distributions were found for the case of reactor heating.

The maximum and minimum temperatures occurring on the cylinder are shown as functions of the rotation parameter λ for both reactor heating and solar heating of the "inert" ($dW = 0$) cylinder in figure 15. These temperatures are not, in general, compatible with the two materials used in the thermodynamic analysis (fig. 3, p. 10).

Specific Weight

Temperature scaling. - There are several materials known which behave like barium titanate but in a different temperature range (refs. 12 and 31 to 34);

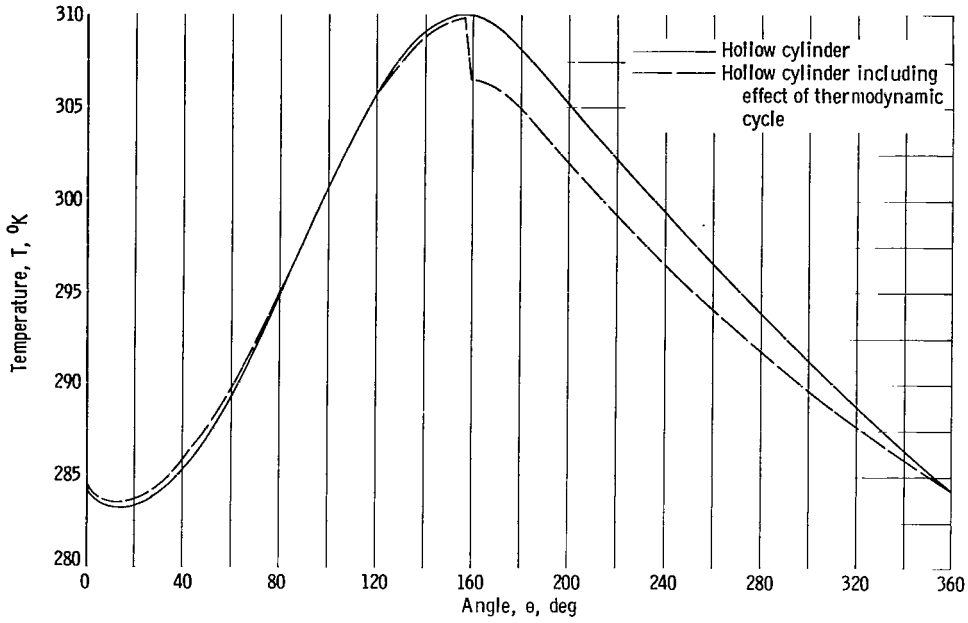

Figure 14. - Temperature distribution for thin-walled hollow cylinder in vicinity of Earth with effect of thermodynamic cycle included. Rotational parameter, 1.0×10^{-9} radian^{-1} $^{o}K^{-3}$; cycle A; material, ferroelectric with characteristic temperature of 273.25° K; correction coefficient, 0; maximum electric field strength, 7.22×10^{6} volts per meter; incident radiant energy from sun, 1390 watts per square meter.

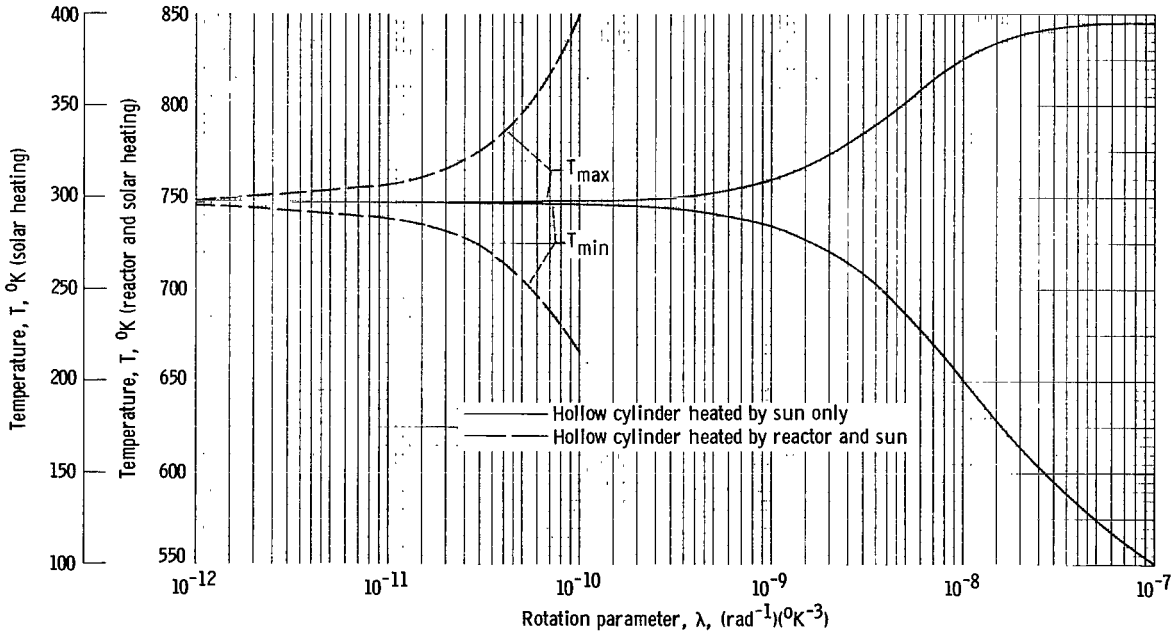

Figure 15. - Maximum and minimum temperatures on thin-walled hollow cylinder heated by reactor only and by both reactor and sun as functions of rotation parameter. Incident power from reactor, 300 000 watts per square meter; incident power from sun, 1390 watts per square meter.

these materials represent a range in T_o (as in eq. 20(b)) from 100° to about 750° K. In order to use the data of figure 15 to obtain estimates of the specific weight of a generator, it is necessary to construct mathematical models for materials that exhibit dielectric properties exactly like those of barium titanate in the temperature ranges calculated. Since T_{max} and T_{min} have been used as parameters in the thermodynamic analysis, it is necessary to preserve the difference $T_{max} - T_{min}$ and the corresponding change in the dielectric constant. This can be done by simply "sliding" the temperature scale of figure 3 (p. 10) up or down to fit the data of figure 15.

For barium titanate, described by equation (20), the term

$$\epsilon(T) = \frac{p}{T - T_o}$$

determines the temperature dependence of the dielectric constant; the characteristic temperature T_o is a convenient reference. The required scaling can be accomplished by simply shifting T_o up or down to fit the desired temperature range and noting that the value of $T_o = 373°$ K was used for figures 6 to 12. Values of $T - T_o$ less than 10° yield values of ϵ that are beyond the maximum values observed experimentally. Consequently, values of $T_{min} - T_o$ less the 10° are not considered in subsequent calculations. In order to evaluate the effect of this temperature scaling, cycle A was analyzed for a range of values of T_o using equations (C2a), (C10), (C11), and (20b). The results for the material similar to barium titanate are presented in figure 16. From figure 6 (p. 19) it can be seen that $T_{max} - T_{min} \approx 20°$ K yields maximum thermal efficiency for most cases; figure 16 shows that for this value of $T_{max} - T_{min}$ the magnitude of the thermal efficiency does not change by more than ±25 percent over the range of temperatures of interest.

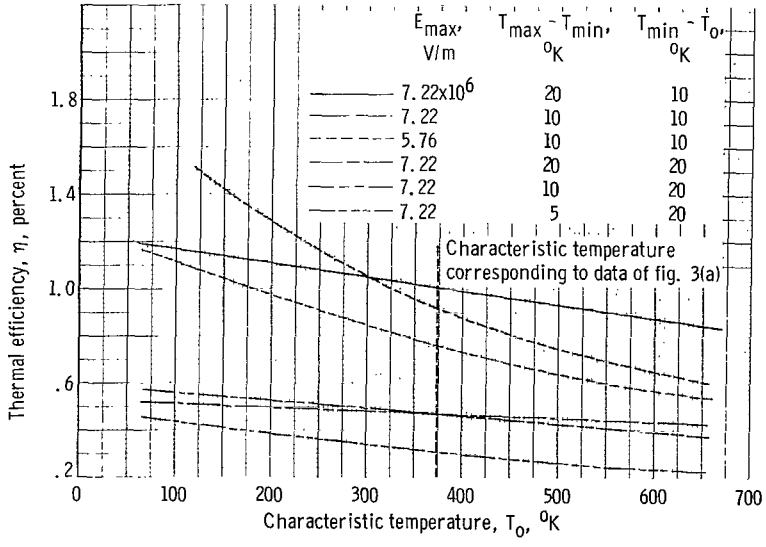

Figure 16. - Effect of absolute temperature on thermal efficiency of cycle A using ferroelectrics similar to barium titanate. Correction coefficient, 0.

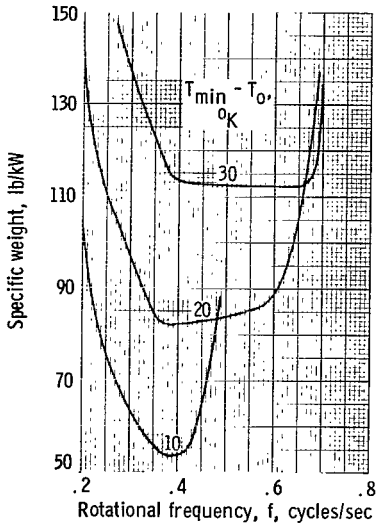

Figure 17. - Typical specific weight curves for cycle B with ferroelectric. Maximum electric field, 7.22×10^6 volts per meter; correction coefficient, 0.

The effect of scaling the temperatures, as shown in figure 16, is small enough that it can be ignored in estimating specific weights. This approximation is of the same order of magnitude as other approximations made thus far in setting up the analysis. Therefore, figures 12(a) and 12(b) can be used directly in a specific weight calculation by simply scaling the endpoint temperatures, as discussed previously, to fit the data of figure 15.

Values of specific weight. - When the temperature scaling technique discussed previously, the data of figures 12(a), 12(b), and (15), and the definition of the rotation parameter λ (eq. (29)) are used, specific weights may be calculated for various combinations of rotational frequency and thickness of the dielectric. Figure 17 shows typical specific weight curves for the material similar to barium titanate using cycle B with solar heating. The dielectric thickness chosen (1.27×10^{-5} m) is about the lower limit that can be achieved with barium titanate without a large decrease in dielectric constant (refs. 35 and 36). The equations for λ and for specific weight can be combined to yield specific weight = $2\pi c\rho^2 \lambda L/\sigma\delta_2 W$. From this form it can be seen that specific weight is directly proportional to dielectric thickness. The lowest specific weights attainable with solar heating are in the neighborhood of 50 to 150 pounds per kilowatt, a value comparable to that of solar cells (ref. 37).

Figure 15 indicates that reactor heating would decrease specific weight of the dielectric material by roughly two orders of magnitude for a given thickness, since specific weight is directly proportional to the λ required to yield a given temperature range and hence specify a value of W. It is necessary, however, to consider the weight of the radiator required to transfer heat from the reactor to the generator.

An estimate of radiator weight for the heat flux used in figure 15 was obtained by using a radiator design computer program (unpublished data obtained from Arthur V. Saule, NASA, Lewis Research Center). This gave a lower limit of roughly 0.25 pound per radiated kilowatt. Assuming a thermal efficiency of 0.75 percent for the generator (optimistic) leads to a minimum radiator weight of 33 pounds per kilowatt output. In this estimate, reactor weight and structural materials needed for the generator have been ignored.

CONCLUDING REMARKS

The performance of a thermoelectrostatic generator has been analyzed in detail. Two thermodynamic cycles have been selected, and mathematical expressions for internal energy and entropy derived. Two materials were selected and their properties approximated by simple mathematical functions. The equations resulting from this mathematical model were solved numerically.

The heat-transfer equations were written for a typical design, heated by the sun and by a nuclear reactor, and solved numerically. The results of this calculation were combined with the results of the thermodynamic analysis to yield the specific weight of the system.

From typical illustrative calculations the following features of generator performance were evident:

1. Barium titanate and materials similar to it are capable of producing three to four times the energy output per unit volume at three to four times the thermal efficiency possible with polyethylene terephthalate.

2. Thermodynamic cycle B is capable of two to three times the energy output at two to three times the thermal efficiency of cycle A.

3. The best possible thermodynamic performance for this generator is a thermal efficiency of 1 to 4 percent and an energy output of 0.5 to 1.5 joules per cubic centimeter of dielectric per cycle, while realistic values are probably lower by at least a factor of five.

4. With solar heating, specific weight of the generator is limited by minimum allowable dielectric thickness and thermodynamic performance of the dielectric to about 50 to 150 pounds per kilowatt.

5. With reactor heating, specific weight is limited by the weight of the radiator needed to transfer heat from the reactor to the generator and by the thermodynamic performance of the dielectric to about 30 to 60 pounds per kilowatt.

6. With currently known materials, this generator is too heavy to be of interest for electric propulsion. As a source of auxiliary power it is comparable, at best, to solar cells in weight. If materials with substantially better characteristics than those considered are found, competitive performance as a power source might be possible.

Lewis Research Center,
National Aeronautics and Space Administration,
Cleveland, Ohio, January 14, 1965.

APPENDIX A

SYMBOLS

A	area, sq m
a,b	generalized endpoints of thermodynamic process
B	constant defined on p. 36
C	capacitance, F
c	specific heat, J/(kg)(^{o}K)
D	electric displacement, C/sq m
E	electric field strength, V/m
E_3/E_2	discharge fraction
f	rotational frequency of cylindrical generator, cycles/sec
K_1	incident radiant energy from sun, 1390 W/sq m
K_2	incident radiant energy from reactor, 300 000 W/sq m
L	thickness of dielectric film, m
P	polarization of dielectric, C/sq m
p	"Curie constant" used in eq. (20b), ^{o}K
Q	thermal energy (heat) per unit volume, J/cu m
q	electric charge, C
S	entropy per unit volume, J/(^{o}K)(cu m)
S_o	entropy per unit volume at zero electric field, J/(^{o}K)(cu m)
T	absolute temperature, ^{o}K
T_o	characteristic temperature for barium titanate, ^{o}K
U	internal energy per unit volume, J/cu m
U_o	internal energy per unit volume at zero electric field, J/cu m
V	voltage, V

W	electric energy output per unit volume per cycle, J/cu m
W'	electric energy (total), J
X,Y,Z	arbitrary variables
α	constant used in eq. (19)
β	constant used in eq. (19), $1/^{o}K$
γ	"correction coefficient" used in eq. (20a), $(V)(m^5)/C^3$
δ_1	surface absorptivity
δ_2	surface emissivity
ϵ	dielectric constant
ϵ_o	permittivity of free space, 8.85×10^{-12} F/m
η	thermal efficiency, percent
θ	angle
σ	Stefan-Boltzmann radiation constant, 5.7×10^{-8} $W/(^{o}K^4)(m^2)$
λ	"rotation parameter" in heat-transfer equations, $1/(^{o}K^3)(rad^1)$
ρ	density, kg/cu m

Subscripts:

a,b	generalized endpoints of thermodynamic process
max	maximum value of variable occurring in course of thermodynamic cycle
min	minimum value of variable occurring in course of thermodynamic cycle
1,2,3, etc.	value of variable at endpoints of thermodynamic cycle; numbers refer to order in which endpoints occur in test discussion (i.e., both cycles begin and end at point 1)
1-2, 2-3, etc.	refer to thermodynamic processes from one endpoint of cycle to next

APPENDIX B

DERIVATION OF THERMODYNAMIC FUNCTIONS

In the following discussion mathematical details of the derivation of the expressions (16a) and (16b) for U and S in terms of the independent variables T and E are presented. The basic equation needed is the first law of thermodynamics:

$$dU = dQ + dW$$

Making the substitution

$$dW = E\, dD$$

gives

$$dU = dQ + E\, dD \tag{B1}$$

For the particular form of D in equation (14b),

$$dD = \frac{\partial D}{\partial \epsilon}\frac{d\epsilon}{dT}\, dT + \frac{\partial D}{\partial E}\, dE \tag{B2}$$

When internal energy is expressed in the form $U = U[\epsilon(T), E]$, equation (B1) can be written

$$dU = dQ + E\left(\frac{\partial D}{\partial \epsilon}\frac{d\epsilon}{dT}\, dT + \frac{\partial D}{\partial E}\, dE\right) = \frac{\partial U}{\partial \epsilon}\frac{d\epsilon}{dT}\, dT + \frac{\partial U}{\partial E}\, dE \tag{B3}$$

Similarly, taking $S = S[\epsilon(T), E]$ leads to

$$\frac{dQ}{T} = dS = \frac{\partial S}{\partial \epsilon}\frac{d\epsilon}{dT}\, dT + \frac{\partial S}{\partial E}\, dE \tag{B4}$$

Since dS is an exact differential, it is necessary that

$$\frac{\partial}{\partial E}\left(\frac{\partial S}{\partial \epsilon}\frac{d\epsilon}{dT}\right) = \frac{\partial}{\partial T}\left(\frac{\partial S}{\partial E}\right) \tag{B5}$$

Solving (B3) for dQ, substituting into (B4), equating coefficients, and applying (B5) yield

$$\frac{\partial}{\partial E}\left[\frac{1}{T}\left(\frac{\partial U}{\partial \epsilon}\frac{d\epsilon}{dT} - E\,\frac{\partial D}{\partial \epsilon}\frac{d\epsilon}{dT}\right)\right] = \frac{\partial}{\partial T}\left[\frac{1}{T}\left(\frac{\partial U}{\partial E} - E\,\frac{\partial D}{\partial E}\right)\right] \tag{B6}$$

Carrying out this operation and noting that

$$\frac{\partial^2 U}{\partial E\, \partial \epsilon} = \frac{\partial^2 U}{\partial \epsilon\, \partial E}$$

$$\frac{\partial^2 D}{\partial E\, \partial \epsilon} = \frac{\partial^2 D}{\partial \epsilon\, \partial E}$$

yield

$$\frac{\partial U}{\partial E} = T \frac{\partial D}{\partial \epsilon} \frac{d\epsilon}{dT} + E \frac{\partial D}{\partial E} \tag{B7}$$

Integration with respect to E gives

$$U = U_o(T) + \int E \frac{\partial D}{\partial E}\, dE + T \int \frac{d\epsilon}{dT} \frac{\partial D}{\partial \epsilon}\, dE \tag{B8}$$

which is equation (16a).

To calculate S, it is noted that (B5) and (B6) yield

$$\frac{\partial S}{\partial E} = \frac{1}{T}\left(\frac{\partial U}{\partial E} - E \frac{\partial D}{\partial E}\right) \tag{B9}$$

and

$$\frac{\partial S}{\partial T} = \frac{1}{T}\left(\frac{\partial U}{\partial \epsilon} \frac{d\epsilon}{dT} - E \frac{\partial D}{\partial \epsilon} \frac{d\epsilon}{dT}\right) \tag{B10}$$

Substituting (B7) into (B9) gives

$$\frac{\partial S}{\partial E} = \frac{\partial D}{\partial \epsilon} \frac{d\epsilon}{dT}$$

so that integration with respect to E gives

$$S = S_o(T) + \int \frac{d\epsilon}{dT} \frac{\partial D}{\partial \epsilon}\, dE \tag{B11}$$

To find $S_o(T)$, it is noted that the condition $E = 0$ reduces (B10) to

$$\frac{dS_o}{dT} = \frac{1}{T} \frac{dU_o}{dT}$$

$$S_o(T) = \int \left(\frac{1}{T} \frac{dU_o}{dT}\right) dT \tag{B12}$$

For a solid material, if it is assumed that ρ and c are independent of temperature, $U_o(T) = \rho c T$, and hence,

$$S_o(T) = \rho c \ln T \tag{B13}$$

Combining equations (B11) and (B13) yields equation (16b).

APPENDIX C

DEVELOPMENT OF FINAL EQUATIONS

In this appendix the explicit equations used in the thermodynamic analysis are derived. The exact equations for U and S are obtained for the two dielectrics considered. The use of these expressions in analyzing the two thermodynamic cycles is then discussed in detail.

Internal Energy and Entropy

For polyethylene terephthalate the expressions for internal energy and entropy are obtained by substituting equation (19) into equations (17c) and (17d) giving

$$U(T,E) = \rho c T + \frac{\epsilon_o E^2}{2}(\alpha + 2\beta T) \tag{C1a}$$

$$S(T,E) = \rho c \ln T + \frac{\epsilon_o E^2}{2}\beta \tag{C1b}$$

For barium titanate, the special case of $\gamma = 0$ is considered first. Equation (20a) may then be rewritten

$$D = \epsilon_o \epsilon(T) E$$

which is the same form as equation (17b). Consequently, the expressions for U and S can be derived by substituting equation (20b) into equations (17c) and (17d):

$$U(T,E) = \rho c T - \frac{\epsilon_o E^2}{2}\frac{p T_o}{(T - T_o)^2} \tag{C2a}$$

$$S(T,E) = \rho c \ln T - \frac{\epsilon_o E^2}{2}\frac{p}{(T - T_o)^2} \tag{C2b}$$

In the general case, $\gamma \neq 0$ and S and U are found by substituting equation (20a) into equations (16a) and (16b). To do this, it is convenient to solve equation (20a) for D (ref. 38):

$$D = \left[\sqrt{\left(\frac{E}{2\gamma}\right)^2 + \left(\frac{1}{3\gamma\epsilon\epsilon_o}\right)^3} + \frac{E}{2\gamma}\right]^{1/3} - \left[\sqrt{\left(\frac{E}{2\gamma}\right)^2 + \left(\frac{1}{3\gamma\epsilon\epsilon_o}\right)^3} - \frac{E}{2\gamma}\right]^{1/3} \tag{C3}$$

where

$$\epsilon = \frac{p}{T - T_o}$$

To complete the calculation of S and U from equations (16a) and (16b) for $\gamma \neq 0$, it is necessary to compute the integrals

$$\int \frac{\partial D}{\partial \epsilon} \, dE$$

and

$$\int E \frac{\partial D}{\partial E} \, dE$$

Equation (C3) yields

$$\frac{\partial D}{\partial \epsilon} = \frac{1}{6\gamma\epsilon_o\epsilon^2} \left\{ \frac{\left[\sqrt{\left(\frac{E}{2\gamma}\right)^2 + \left(\frac{1}{3\gamma\epsilon\epsilon_o}\right)^3} + \frac{E}{2\gamma} \right]^{2/3} - \left[\sqrt{\left(\frac{E}{2\gamma}\right)^2 + \left(\frac{1}{3\gamma\epsilon\epsilon_o}\right)^3} - \frac{E}{2\gamma} \right]^{2/3}}{\sqrt{\left(\frac{E}{2\gamma}\right)^2 + \left(\frac{1}{3\gamma\epsilon\epsilon_o}\right)^3}} \right\} \tag{C4}$$

Making the substitutions

$$X = \frac{E}{2\gamma}$$

and

$$B^2 = \left(\frac{1}{3\gamma\epsilon_o\epsilon}\right)^3$$

in equation (C4), the integral reduces to the form

$$\int \frac{\partial D}{\partial \epsilon} \, dE = \frac{1}{3\epsilon_o\epsilon^2} \left[\int \frac{\left(\sqrt{X^2 + B^2} + X\right)^{2/3}}{\sqrt{X^2 + B^2}} \, dX - \int \frac{\left(\sqrt{X^2 + B^2} - X\right)^{2/3}}{\sqrt{X^2 + B^2}} \, dX \right] \tag{C5}$$

When the substitutions $X = BY$ in the first integral and $X = -BZ$ in the second are made, equation (C5) reduces to a standard form in reference 39. This leads to the result

$$\int \frac{\partial D}{\partial \epsilon}\, dE = \frac{1}{2\epsilon_o \epsilon^2} \left\{ \left[\sqrt{\left(\frac{E}{2\gamma}\right)^2 + \left(\frac{1}{3\gamma\epsilon\epsilon_o}\right)^3} + \frac{E}{2\gamma} \right]^{2/3} + \left[\sqrt{\left(\frac{E}{2\gamma}\right) + \left(\frac{1}{3\gamma\epsilon\epsilon_o}\right)^3} - \frac{E}{2\gamma} \right]^{2/3} \right\} \tag{C6}$$

To find $\int E \frac{\partial D}{\partial E}\, dE$, it is noted that an integration by parts gives

$$\int E \frac{\partial D}{\partial E}\, dE = ED - \int D\, dE \tag{C7}$$

If equation (C3) and the same substitutions as before are used, the remaining integral takes the form

$$\int D\, dE = 2\gamma \left[\int \left(\sqrt{X^2 + B^2} + X \right)^{1/3} dX - \int \left(\sqrt{X^2 + B^2} - X \right)^{1/3} dX \right]$$

Evaluating this equation (ref. 39) and using equations (C3) and (C7) lead to

$$\int E \frac{\partial D}{\partial E}\, dE = -\frac{1}{8} ED + \frac{3}{4} \gamma \sqrt{\left(\frac{E}{2\gamma}\right)^2 + \left(\frac{1}{3\gamma\epsilon\epsilon_o}\right)^3} \left\{ \left[\sqrt{\left(\frac{E}{2\gamma}\right)^2 + \frac{1}{3\gamma\epsilon\epsilon_o}\right)^3} + \frac{E}{2\gamma} \right]^{1/3} + \left[\sqrt{\left(\frac{E}{2\gamma}\right)^2 + \left(\frac{1}{3\gamma\epsilon\epsilon_o}\right)^3} - \frac{E}{2\gamma} \right]^{1/3} \right\} \tag{C8}$$

Noting that $\frac{d\epsilon}{dT} = -\frac{\epsilon^2}{p}$ and substituting equations (C6) and (C8) into equations (16a) and (16b) yield

$$\begin{aligned} U(T,E) = \rho c T &- \frac{E}{8} \left\{ \left[\sqrt{\left(\frac{E}{2\gamma}\right)^2 + \left(\frac{1}{3\gamma\epsilon\epsilon_o}\right)^3} + \frac{E}{2\gamma} \right]^{1/3} \right. \\ &\left. - \left[\sqrt{\left(\frac{E}{2\gamma}\right)^2 + \left(\frac{1}{3\gamma\epsilon\epsilon_o}\right)^3} - \frac{E}{2\gamma} \right]^{1/3} \right\} + \frac{3}{4} \gamma \sqrt{\left(\frac{E}{2\gamma}\right)^2 + \left(\frac{1}{3\gamma\epsilon\epsilon_o}\right)^3} \\ &\times \left\{ \left[\sqrt{\left(\frac{E}{2\gamma}\right)^2 + \left(\frac{1}{3\gamma\epsilon\epsilon_o}\right)^3} + \frac{E}{2\gamma} \right]^{1/3} + \left[\sqrt{\left(\frac{E}{2\gamma}\right)^2 + \left(\frac{1}{3\gamma\epsilon\epsilon_o}\right)^3} - \frac{E}{2\gamma} \right]^{1/3} \right\} \\ &- \frac{T}{2\epsilon_o p} \left\{ \left[\sqrt{\left(\frac{E}{2\gamma}\right)^2 + \left(\frac{1}{3\gamma\epsilon\epsilon_o}\right)^3} + \frac{E}{2\gamma} \right]^{2/3} + \left[\sqrt{\left(\frac{E}{2\gamma}\right)^2 + \left(\frac{1}{3\gamma\epsilon\epsilon_o}\right)^3} - \frac{E}{2\gamma} \right]^{2/3} \right\} \end{aligned} \tag{C9a}$$

$$S(T,E) = \rho c \ln T - \frac{1}{2\epsilon_o p}\left\{\left[\sqrt{\left(\frac{E}{2\gamma}\right)^2 + \left(\frac{1}{3\gamma\epsilon\epsilon_o}\right)^3} + \frac{E}{2\gamma}\right]^{2/3} + \left[\sqrt{\left(\frac{E}{2\gamma}\right)^2 + \left(\frac{1}{3\gamma\epsilon\epsilon_o}\right)^3} - \frac{E}{2\gamma}\right]^{2/3}\right\} \qquad \text{(C9b)}$$

Defining Equations for Cycle A

In the following discussion, the endpoints of the cycle are labelled 1, 2, 3, respectively, and the processes joining them are labelled 1-2, 2-3, and 3-1 (constant charge, adiabatic, constant field), respectively. When equations (11) to (13) are used, cycle A may be analyzed as follows:

$$\Delta Q_{1-2} = U(T_2,E_2) - U(T_1,E_1) \qquad \text{(C10a)}$$

$$\Delta W_{2-3} = U(T_3,E_3) - U(T_2,E_2) \qquad \text{(C10b)}$$

$$\Delta Q_{3-1} = U(T_1,E_1) - U(T_3,E_3) - E_1\left[D(T_1,E_1) - D(T_3,E_3)\right] \qquad \text{(C10c)}$$

$$\Delta W_{3-1} = E_1\left[D(T_1,E_1) - D(T_3,E_3)\right] \qquad \text{(C10d)}$$

where

$$D(T_2,E_2) = D(T_1,E_1) \qquad \text{(C11a)}$$

$$S(T_3,E_3) = S(T_2,E_2) \qquad \text{(C11b)}$$

$$E_1 = E_3 \qquad \text{(C11c)}$$

Equations (C11) yield E_1, E_3, and T_3 since T_1, T_2, and E_2 are specified.

In order to calculate the thermal efficiency, the usual definition $\eta = \frac{\text{heat in - heat out}}{\text{heat in}}$ is used. For a material whose dielectric constant decreases with increasing temperature, heat must be added during the first (constant charge) process in order to have $E_2 > E_1$ as required. Therefore, ΔQ_{1-2} = heat in and ΔQ_{3-1} = heat rejected, which leads to the expression

$$\frac{U(T_2,E_2) - U(T_3,E_3) - E_1[D(T_1,E_1) - D(T_3,E_3)]}{U(T_2,E_2) - U(T_1,E_1)} \qquad \text{(C12a)}$$

For a material whose dielectric constant increases with increasing temperature, heat must be rejected during the constant-charge process; hence,

ΔQ_{1-2} = heat rejected and ΔQ_{3-1} = heat added. This leads to the expression

$$\eta = \frac{U(T_2,E_2) - U(T_3,E_3) - E_1[D(T_1,E_1) - D(T_3,E_3)]}{U(T_1,E_1) - U(T_3,E_3) - E_1[D(T_1,E_1) - D(T_3,E_3)]} \qquad \text{(C12b)}$$

Cycle B

In the following discussion, the endpoints of the cycle will be labelled 1, 2, 3, and 4, respectively, and the processes joining them will be labelled 1-2, 2-3, etc. (constant charge, adiabatic, constant charge, adiabatic, respectively). Equations (11) to (13) lead to the following equations:

$$\Delta Q_{1-2} = U(T_2,E_2) - U(T_1,E_1) \qquad \text{(C13a)}$$

$$\Delta W_{2-3} = U(T_3,E_3) - U(T_2,E_2) \qquad \text{(C13b)}$$

$$\Delta Q_{3-4} = U(T_4,E_4) - U(T_3,E_3) \qquad \text{(C13c)}$$

$$\Delta W_{4-1} = U(T_1,E_1) - U(T_4,E_4) \qquad \text{(C13d)}$$

where

$$D(T_1,E_1) = D(T_2,E_2) \qquad \text{(C14a)}$$

$$S(T_3,E_3) = S(T_2,E_2) \qquad \text{(C14b)}$$

$$D(T_4,E_4) = D(T_3,E_3) \qquad \text{(C14c)}$$

$$S(T_1,E_1) = S(T_4,E_4) \qquad \text{(C14d)}$$

If equation (16a) and the equation for D appropriate to the dielectric being considered are used, equations (C14) can be solved for T_1, T_3, E_1, and E_4 since T_2, T_4, E_2, and E_3 are specified.

Thermal efficiency can be calculated from equations (C13). The arguments used in the efficiency calculation for cycle A apply equally well here. Therefore, the use of a material whose dielectric constant decreases with increasing temperature requires that ΔQ_{1-2} = heat added and ΔQ_{3-4} = heat rejected; hence,

$$\eta = \frac{U(T_2,E_2) - U(T_1,E_1) + U(T_4,E_4) - U(T_3,E_3)}{U(T_2,E_2) - U(T_1,E_1)} \qquad \text{(C15a)}$$

If a material whose dielectric constant increases with temperature is used, ΔQ_{1-2} = heat rejected and ΔQ_{3-4} = heat added; hence,

$$\eta = \frac{U(T_2,E_2) - U(T_1,E_1) + U(T_4,E_4) - U(T_3,E_3)}{U(T_4,E_4) - U(T_3,E_3)} \qquad \text{(C15b)}$$

Table II gives the densities and specific heats used for the analysis.

TABLE II. - DENSITIES AND SPECIFIC HEATS OF TEST MATERIALS

Density, ρ		Specific heat, c	
kg/m^3	g/cm^3	$J/(kg)(^oK)$	cal/g
Barium titanate			
[a]5500	[a]5.5	[a]418.6	[a]0.1
Polyethylene terephthalate			
[b]1380	[b]1.38	[c]1300	[c]0.31

[a]Reference 24.
[b]Reference 14.
[c]Reference 40.

APPENDIX D

HEAT-TRANSFER CALCULATIONS

In this section, the equations used to describe the energy balance for the cylindrical generator design are presented. Two heat sources, the sun and a nuclear reactor, are discussed. Finally, the effect of the transfer of electrical energy is included for the special case of cycle A with barium titanate as the dielectric.

Cylinder - Solar Heating

In setting up the heat-transfer equation for a hollow cylinder heated by solar radiation (fig. 1(a), p. 2), the following approximations are used:

(1) Heat conduction along the dielectric film is ignored; radiation is the only heat-transfer mechanism considered.

(2) No heat is transferred to the interior of the cylinder by radiation; the inner electrode is assumed a perfect reflector.

(3) Only thermal properties of the dielectric are considered.

(4) Uniform rotational frequency is assumed.

The first two of these assumptions are discussed in detail in reference 2.

These four approximations lead to the following description of the heat-transfer process (ref. 2):

$$\frac{dT}{d\theta} = \lambda \frac{\delta_1}{\delta_2} \frac{K_1}{\sigma} \sin \theta - \lambda T^4 \qquad 0 < \theta \pi \tag{D1a}$$

$$\frac{dT}{d\theta} = - \lambda T^4 \qquad \pi \leq \theta \leq 2\pi \tag{D1b}$$

where

$\lambda = \sigma\delta_2/2\pi fL\rho C$, $K_1 = 1390$ watts per square meter (solar constant at Earth's orbit), and $0 \leq \theta \leq \pi$ corresponds to the sunlit side. In order to solve these equations, it is necessary to choose an initial temperature at an initial angle. The solution to one equation provides boundary conditions for the next as the "critical" angles $\theta = 0$ and $\theta = \pi$ are encountered.

Cylinder - Reactor Heating

Figure 18 shows the model used to determine the effect of heating the cylinder with a reactor. Heat is transferred from the reactor to the cylinder

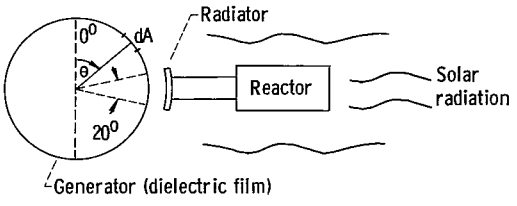

Figure 18. - Model used to determine effect of heating a cylinder with a reactor.

by the radiator. In the interest of minimum weight, the radiator was assumed to yield a heat flux density of 300 000 watts per square meter, which corresponds to a blackbody temperature of 1520° K. This temperature is a practical upper limit for materials presently under consideration for use in a radiator (ref. 41). The maximum temperatures of the dielectric compatible with known ferroelectric materials is in the range of 700° to 800° K (ref. 34). The desired heat flux density and the desired temperature range of the dielectric dictate that the radiator subtend an arc of approximately 20°, as shown in figure 18.

When subject to the same assumptions used for solar testing, this system can be described as follows:

$$\frac{dT}{d\theta} = \lambda \frac{\delta_1}{\delta_2} \frac{K_1}{\sigma} \sin\theta - \lambda T \qquad 0 < \theta < 80^\circ;\ 100^\circ < \theta < 180^\circ \qquad \text{(D2a)}$$

$$\frac{dT}{d\theta} = \lambda \frac{\delta_1}{\delta_2} \frac{K_2}{\sigma} \sin\theta \qquad 80^\circ < \theta\ 100^\circ \qquad \text{(D2b)}$$

(for $T \ll 1520^\circ$ K = T radiator)

$$\frac{dT}{d\theta} = -\lambda T^4 \qquad 180^\circ < \theta < 360^\circ \qquad \text{(D2c)}$$

Effect of Thermodynamic Cycle

In order to determine the change in temperature distribution on the cylinder (given by eqs. (D1a) and (D1b)) caused by the execution of a thermodynamic cycle, it is necessary to modify the mathematical description of the dielectric since the temperature range on the cylinder will not in general match that in figure 3 (p. 10) (viz, 350° to 400° K for polyethylene terephthalate and 385° to 450° K, above Curie temperature, for barium titanate). This was done by considering a hypothetical material with the properties of barium titanate in a different temperature range. The temperature scaling technique described in the text was used.

In the interest of simplicity, cycle A was used in this analysis with a dielectric having properties similar to those of barium titanate (temperatures scaled). Equations (C2a), (C2b), (C10), and (C11) describe the thermodynamic cycle.

Heat is transferred by radiation; hence, an equation of the form $dQ_{thermodynamic} = dQ_{radiated}$ must be satisfied. Because of this additional constraint on the temperature, only two variables can be specified arbitrarily. These were E_{max} and λ. An additional stipulation was that $T_{min} - T_o = 10^\circ$ K

so as to guarantee a maximum variation of dielectric constant and hence a maximum effect on the temperature distribution of the cylinder. Writing equation (C10a) in differential form leads to the equation

$$\frac{dT}{d\theta} = \lambda \frac{\delta_1}{\delta_2} \frac{K_1}{\sigma} \sin \theta - \lambda T^4 \qquad \theta_1 \leq \theta \leq \theta_2 \qquad \text{(D3a)}$$

(which describes process 1-2) where θ_1 is the angle at which T_{min} occurs and θ_2 is the angle at which T_{max} occurs.

If an adiabatic (and isentropic) process (process 2-3) is to be achieved in a practical system, it must be done quickly, that is, while the generator rotates through a small angle. Therefore, it was arbitrarily assumed that the generator rotates from θ_2 to $\theta_2 + 2^\circ$ during this process. (The calculation was done for several choices of this angle; results were very nearly identical for angles ranging from 0° to 5°.) The temperature T_3, occurring at θ_3, is calculated from equation (23):

$$\frac{\epsilon_o p E_2^2}{2\rho c} \left(\frac{1}{T_2 - T_o} \right)^2 \left[1 - \left(\frac{T_1 - T_o}{T_3 - T_o} \right)^2 \right] + \ln \frac{T_3}{T_2} = 0 \qquad \text{(D3b)}$$

Process 3-1 (constant field) is described by putting equation (C10c) in differential form, which gives

$$\left[1 + \frac{\epsilon_o p E_2^2}{\rho c} \left(\frac{T_1 - T_o}{T_2 - T_o} \right)^2 \frac{T}{(T - T_o)^3} \right] \frac{dT}{d\theta} = \lambda \frac{\delta_1}{\delta_2} \frac{K_1}{\sigma} \sin \theta - \lambda T^4 \qquad \begin{cases} \theta_3 \leq \theta \leq \pi \\ 0 \leq \theta \leq \theta_1 \end{cases} \qquad \text{(D3c)}$$

$$= - \lambda T^4 \qquad \pi \leq \theta \leq 2\pi$$

Equations (D3) were solved numerically. It is necessary to select specific values for θ_1 and θ_2, at which angles $T_1 = T_{min}$ and $T_2 = T_{max}$ must occur, in order that the equations can be solved. These arbitrary initial choices will not, in general, be correct (i.e., T_{min} and T_{max} will occur at angles other than those selected); hence, an iteration process is needed to find the correct values of θ_1 and θ_2, at which T_{min} and T_{max} occur, and to readjust the value of T_o to guarantee that

$$T_{min} - T_o = 10^\circ \text{ K}$$

as originally specified. Equations (C10) and (C12a) then yield thermal efficiency, net energy output per cycle, etc.

REFERENCES

1. Moeckel, W. E.: Fast Interplanetary Missions With Low-Thrust Propulsion Systems. NASA TR R-79, 1960.

2. Beam, Benjamin H.: An Exploratory Study of Thermoelectrostatic Power Generation for Space Flight Applications. NASA TN D-336, 1960.

3. Gignoux, Dominique: Constant Oblique Field Electrostatic Generator. Paper 2556-62, ARS, 1962.

4. Denholm, A. S.; Trump, J. G.; and Gale, A. J.: High Voltage Generation in Space: The Parametric Electrostatic Machine, Energy Conversion for Space Power. Prog. in Astronautics and Rocketry, Vol. 3, Academic Press, Inc., 1961, pp. 767-779.

5. Breaux, O. P.: Electrostatic Power Generation for Space Propulsion. Elec. Eng., vol. 78, no. 11, Nov. 1959, pp. 1102-1104.

6. Trump, John G.: Electrostatic Sources of Electric Power. Elec. Eng., vol. 66, no. 6, June 1947, pp. 525-534.

7. Anon.: Silicon Controlled Rectifier Manual. Second ed., General Electric Co., 1961.

8. Anon.: Ferroelectrics Generate Power. Electronics, vol. 32, no. 51, Dec. 18, 1959, pp. 88-90.

9. Kovit, Bernard: Ferroelectric Power Source for Space Vehicles. Space/Aeronautics, vol. 33, no. 3, Mar. 1960, pp. 131-133.

10. Fröhlich, H.: Theory of Dielectrics. Oxford Univ. Press, 1949, pp. 9-13; 161.

11. Karchevskii, A. I.: Electrocaloric Effect in Polycrystalline Barium Titanate. Soviet Phys.-Solid State, vol. 3, no. 10, Apr. 1962, pp. 2249-2254.

12. Shirane, G.; Jona, F.; and Pepinsky, R.: Some Aspects of Ferroelectricity. Proc. IRE, vol. 43, no. 12, Dec. 1955, pp. 1738-1793.

13. Von Hippel, A.: Ferroelectricity, Domain Structure, and Phase Transitions of Barium Titanate. Rev. Mod. Phys., vol. 22, no. 3, July 1950, pp. 221-237.

14. Reddish, Wilson: The Dielectric Properties of Polyethylene Terephthalate. Trans. Faraday Soc., vol. 46, 1950, pp. 459-475.

15. Roberts, Shepard: Dielectric and Piezoelectric Properties of Barium Titanate. Phys. Rev., vol. 71, no. 12, June 15, 1947, pp. 890-895.

16. Inuishi, Y.; and Powers, D. A.: Electric Breakdown and Conduction Through Mylar Films. J. Appl. Phys., vol. 28, no. 9, Sept. 1957, pp. 1017-1022.

17. Fang, P. H.; and Brower, W. S.: Temperature Dependence of the Breakdown Field of Barium Titanate. Phys. Rev., vol. 113, no. 2, Jan. 15, 1959, pp. 456-458.

18. Kline, L. V.; Marco, S. M.; and Starkey, W. L.: Work Capacities of Energy Storage Systems on the Basis of Unit Weight and Unit Volume. ASME Trans., vol. 80, no. 4, May 1958, pp. 909-914.

19. Lupfer, D. A.: Electrical Characteristics of High Density, High Purity Titanate Ceramics. Paper No. 15/P/1544, Second United Nations Int. Conf. on the Peaceful Uses of Atomic Energy, vol. 32, 1958, pp. 457-460.

20. Kraus, J. D.: Electromagnetics. McGraw-Hill Book Co., Inc., 1953, p. 237.

21. Drougard, M. E.; and Young, D. R.: Dielectric Constant Behavior of Single-Domain, Single Crystals of Barium Titanate in the Vicinity of the Curie Point. Phys. Rev., vol. 95, no. 5, Sept. 1, 1954, pp. 1152-1153.

22. Drougard, M. E.; and Huibregtse, E. J.: The Effect of an Electric Field on the Transitions of Barium Titanate. IBM J. Res. & Dev., vol. 1, no. 4, Oct. 1957, pp. 318-329.

23. Merz, Walter J.: Double Hysteresis Loop of $BaTiO_3$ at the Curie Point. Phys. Rev., vol. 91, no. 3, Aug. 1, 1953, pp. 513-517.

24. Childress, J. D.: Application of a Ferroelectric Material in an Energy Conversion Device. J. Appl. Phys., vol. 33, no. 5, May 1962, pp. 1793-1798.

25. Khodakov, A. L.: Dielectric Properties of Finely Dispersed Barium Titanate. Soviet Phys.-Solid State, vol. 2, no. 9, Mar. 1961, pp. 1904-1907.

26. Diamond, Howard: Variation of Permittivity with Electric Field in Perovskite-Like Ferroelectrics. J. Appl. Phys., vol. 32, no. 5, May 1961, pp. 909-915.

27. Devonshire, A. F.: Theory of Barium Titanate, pt. I. Phil. Mag., ser. 7, vol. 40, no. 309, Oct. 1949, pp. 1040-1063.

28. Drougard, M. E.; Landauer, R.; and Young, D. R.: Dielectric Behavior of Barium Titanate in the Paraelectric State. Phys. Rev., vol. 98, no. 4, May 15, 1955, pp. 1010-1014.

29. Clingman, W. H.; and Moore, R. G., Jr.: Application of Ferroelectricity to Energy Conversion Processes. J. Appl. Phys., vol. 32, no. 4, Apr. 1961, pp. 675-681.

30. Scarborough, James Blaine: Numerical Mathematical Analysis. Fourth ed., Johns Hopkins Press, 1958, pp. 192-207.

31. Bokov, V. A.; and Myl'nikova, I. E.: Ferroelectric Properties of Monocrystals of New Perovskite Compounds. Soviet Phys.-Solid State, vol. 2, no. 11, May 1961, pp. 2428-2432.

32. Smolenskii, G. A.; Isupov, V. A.; Agranovskaya, A. I., and Krainik, N. M.: New Ferroelectrics of Complex Composition, IV. Soviet Phys.-Solid State, vol. 2, no. 11, May 1961, pp. 2651-2654.

33. Pulvari, Charles F.: Ferroelectricity. Phys. Rev., vol. 120, no. 5, Dec. 1, 1960, pp. 1670-1673.

34. Matthias, B. T.; and Remeika, J. P.: Dielectric Properties of Sodium and and Potassium Niobates. Phys. Rev., vol. 82, no. 5, June 1, 1951, pp. 727-729.

35. Yamanaka, S.: Ferroelectric Thin Film Deposited by Electrophoresis. Electrotechnical J. of Japan, vol. 4, no. 4, Dec. 1958, pp. 132-136.

36. Feldman, Charles: Formation of Thin Films of $BaTiO_3$ by Evaporation. Rev. Sci. Instru., vol. 26, no. 5, May 1955, pp. 463-466.

37. Cherry, W. R.: Solar Cells and the Applications Engineer. Astronautics and Aerospace Eng., vol. 1, no. 4, May 1963, pp. 54-57.

38. Burington, Richard Stevens: Handbook of Mathematical Tables and Formulas. Handbook Publ., Inc., Sandusky (Ohio), 1940, p. 7.

39. Bois, Petit: Tables of Indefinite Integrals. Dover Publ. Inc., 1961, pp. 110-111.

40. Anon.: Mylar Polyester Film. Bull. M-1B, DuPont de Nemours, (E. I.) & Co., 1963.

41. Evvard, J. C.: A Viewpoint on Space Propulsion and Power-Generation Systems. Proc. Int. Symposium on Space Tech. and Sci., Tokyo (Japan), Aug. 27-31, 1962, Japan Publ. Trading Co., 1963, pp. 417-426.

2/22/85

"The aeronautical and space activities of the United States shall be conducted so as to contribute . . . to the expansion of human knowledge of phenomena in the atmosphere and space. The Administration shall provide for the widest practicable and appropriate dissemination of information concerning its activities and the results thereof."

—NATIONAL AERONAUTICS AND SPACE ACT OF 1958

NASA SCIENTIFIC AND TECHNICAL PUBLICATIONS

TECHNICAL REPORTS: Scientific and technical information considered important, complete, and a lasting contribution to existing knowledge.

TECHNICAL NOTES: Information less broad in scope but nevertheless of importance as a contribution to existing knowledge.

TECHNICAL MEMORANDUMS: Information receiving limited distribution because of preliminary data, security classification, or other reasons.

CONTRACTOR REPORTS: Technical information generated in connection with a NASA contract or grant and released under NASA auspices.

TECHNICAL TRANSLATIONS: Information published in a foreign language considered to merit NASA distribution in English.

TECHNICAL REPRINTS: Information derived from NASA activities and initially published in the form of journal articles.

SPECIAL PUBLICATIONS: Information derived from or of value to NASA activities but not necessarily reporting the results of individual NASA-programmed scientific efforts. Publications include conference proceedings, monographs, data compilations, handbooks, sourcebooks, and special bibliographies.

Details on the availability of these publications may be obtained from:

SCIENTIFIC AND TECHNICAL INFORMATION DIVISION

NATIONAL AERONAUTICS AND SPACE ADMINISTRATION

Washington, D.C. 20546